

**Determining which octopamine receptor links appetite and fluctuating
trehalose levels in the honey bee**

by

SALEH GHANEM

Supervisor: Prof. Christopher Mayack

Submitted to the Graduate School of Engineering and Natural sciences
in partial fulfilment of
the requirements for the degree of Master of Science

Sabanci University

July 2021

SALEH GHANEM 2021 ©
All Rights Reserved

ABSTRACT

Determining which octopamine receptor links appetite and fluctuating trehalose levels in the honey bee

SALEH GHANEM

Molecular Biology, Genetics and Bioengineering, MSc Thesis July 2021

Thesis Supervisor: Asst. Prof. Christopher Mayack

Keywords: OA, GCMS, CRISPR/Cas9, HPLC, AmOct, Fura-2

For foraging honey bees, fluctuating energy demands are high because at times they must sustain flight which is energetically expensive. Therefore, they provide an ideal model for studying how an organism can precisely regulate their appetite. Trehalose is the main sugar found in the hemolymph of the honey bee. The fluctuating level of this sugar was investigated to determine if there is a connection with the octopamine (OA) level in the brain. First, we manipulated the hemolymph sugar levels using thorax sugar injections and found that they were most effective in the forager age class, which corresponded with the largest changes in appetite across all age classes. The lowering of trehalose levels corresponded with an increase in octopamine levels in the honey bee brain. The appetite regulation observed was independent of the glucose-insulin signaling pathway as indicated by ILP1 and ILP2 gene expression. Based on these results, I designed a CRISPR-cas9 plasmid to knockdown the octopamine beta receptor subtype-2 to determine its role in appetite regulation. The fura-2 biosensor measured calcium signaling and the presence of octopamine receptors in a newly established Ame711 cell line. In future work, I will test baculovirus' transduction efficiency using the Ame711 honey bee cell line to determine its transduction efficiency before using it as a vector to deliver the CRISPR-cas9 complex *in vivo*. In summary, using these newly developed tools, identifying whether there is a causal link between octopamine and appetite regulation in the honey bee will be possible.

ÖZET

Bal arısında iřtah ile dalgalanan trehaloz seviyeleri arasındaki baęlantının hangi oktopamin reseptörü olduęunun belirlenmesi

SALEH GHANEM

Moleküler Biyoloji, Genetik ve Biyomühendislik, Yüksek Lisans Tezi, 2021

Tez Danıřmanı: Dr.Öęr. Üyesi Christopher Mayack

Anahtar Kelimeler: OA, GCMS, CRISPR/Cas9, HPLC, AmOct, Fura-2

Tarlacı bal arıları enerji tüketimi fazla olan uęma eylemini gerçekleřtirdikleri için enerji gereksinimleri yüksek arılardır. Bu nedenle bu bal arıları iřtah mekanizmasının çalışılabilmesi için iyi bir model organizmadırlar. Trehaloz, bal arısının hemolenfinde bulunan ana şekerdir. Trehalozun hemolenfte dalgalanan seviyeleri, beyinde oktopamin (OA) ile bir baęlantı olup olmadığını belirlemek için araştırıldı. İlk olarak, toraks şekeri enjeksiyonu kullanarak hemolenf şeker seviyelerini manipüle ettik ve bu manipölasyonun tüm yař sınıflarında iřtahta en büyük deęişikliklere sebep olduęunu, en büyük deęişimin ise tarlacı arılarda meydana geldięini gözlemledik. Trehaloz seviyelerinin düşürülmesi, bal arısı beyindeki oktopamin seviyelerinde bir artışa neden olmuřtur. İřtah mekanizmasının, ILP1 ve ILP2 gen ekspresyonu ile belirtildięi gibi, glukoz-insülin sinyal yolundan baęımsız olduęunu gözlemledik. Bu sonuçlara dayanarak, iřtah düzenlemesindeki rolünü belirlemek için oktopamin beta reseptörü alt tür 2'nin knockdown edilmesi için bir CRISPR-cas9 plazmidi tasarladım. Fura-2 biyosensörü, yeni elde edilmiř bir Ame711 hücre hattında kalsiyum sinyalini ve oktopamin reseptörlerinin varlıęını ölçmüřtür. Gelecekteki çalışmalarda, CRISPR-cas9 kompleksini in vivo teslimi için bir vektör olarak kullanmadan önce transdüksiyon verimlilięini belirlemek için Ame711 bal arısı hücre hattını kullanarak bakulovirüsün transdüksiyon verimlilięini test edeceęim. Özetle, yeni geliřtirilen bu araçları kullanarak, bal arısında oktopamin ile iřtah düzenlemesi arasında nedensel bir baęlantı olup olmadığını tespit etmek mümkün olacaktır.

ACKNOWLEDGEMENTS

I would like to extend my sincerest and utmost thanks to my thesis advisor Prof. Christopher Mayack for his unwavering support and guidance throughout the duration of my master's studies. His motivation and perseverance are truly an inspiration to me. Being a part of the Mayack Lab has enriched my drive, curiosity, and critical thinking skills. I am also thankful to my jury members Prof. Ozlem Kutlu and Prof. Robert L. Broadrup for their feedback on my thesis.

I would like to thank the members of our lab: Irem Akulku, Kubra Guzle, Hasim Hakanoglu and Mert Ozle. From these amazing individuals, I would like to convey my appreciation to Irem, as she was always willing and eager to help out in whatever I asked of her, and more importantly she was there for me as a friend. I would like to thank Kubra, without whom I would not have been able to carry out this study. I would like to thank Prof. Emrah and Yusuf Altun for their guidance and support. This path would have been impossible without my beloved Bissan, or my dear friends Anas, Mesfer and Aboud.

I am also grateful to my beloved family for their support and belief in me. I would not have been able to fulfill my studies without my dear family, from my father's guidance, to my mother's love, to my siblings' faith in me. From the bottom of my heart, Thank you.

Finally, I would like to acknowledge Tubitak for the financial support they provided. This study was supported by the TUBITAK grant entitled "Bal arısı iřtahının glikoz insülin sinyal yolađından bađımsız regülasyonu" Number: 3501.

To my Family...

Table of Contents

1. INTRODUCTION	1
1.1 General overview	1
1.2 Trehalose in relation with appetite.....	2
1.3 Octopamine receptors in the honey bee brain.....	3
1.4 CRISPR-Cas9	5
1.5 Cell lines	9
2. AIM OF THE STUDY	11
3. MATERIALS & METHODS	12
3.1 Materials	12
3.1.1 Chemicals.....	12
3.1.2 Equipment.....	12
3.1.3 Molecular biology kits.....	12
3.1.4 Software, websites, and computer-based applications.....	12
3.2 Methods	13
3.2.1 Collection, marking and injection of the bees with different sugars	13
3.2.3. Quantification of sugars in hemolymph using GCMS.....	15
3.2.3.1. Sample preparation & lyophilization	15
3.2.3.2 Derivatization.....	16
3.2.3.3 GC-MS analysis	16
3.2.1.1 Dissections	17
3.2.2 Biogenic amine analysis of bee brains.....	Error! Bookmark not defined.
3.2.4 qPCR gene expression analysis of ILP1-2.....	18
3.2.5 CRISPR-cas9 knockdowns of octopamine receptors in the bee brain.....	19

3.2.5.1. Cell culturing and characterization of the cell line	19
3.2.5.2 Calcium cell imaging	20
3.2.5.3. Plasmid design	21
Transduction	27
4. Results	28
5. Discussion	34
5.1 Sugar level manipulation confirmation.....	34
5.2 Fura-2 imaging.....	38
Bibliography.....	41
Appendix A – Chemicals	48
Appendix B – Equipment	49
Appendix C – Biological Kits.....	50
Appendix D - Supplemental Figures	51

LIST OF TABLES

Table 3.1 List of software, websites, and computer-based applications.....	11
Table 3.2 Volumes of each sugar to be added to the external standard stocks.....	14
Table 3.3 Composition of the calcium-containing physiological solution.....	20

LIST OF FIGURES

Figure 1 Trehalose composed of two glucose molecules bound together	3
Figure 2 CRISPR Cas9 discovery, the mechanism behind bacterial immunity.....	6
Figure 3 The various approaches that the Cas9 enzyme may be used to create various genetic edits.....	7
Figure 4 Depiction of various ways that Cas9 could be introduced into cells	8
Figure 5 Honey bee brain dissections on dry ice.....	18
Figure 6 Light microscope images of Ame711, 40X zoom.....	20
Figure 7 Initial proposed plasmid constructs A and B.....	22
Figure 8. Benchling PAM and gRNA sequence output.....	24
Figure 9 Schematic depicting how T2A leads to two separate proteins, using a single promotor.....	25
Figure 10 Schematic of the de novo designed, finalized plasmid.....	25
Figure 11 Plasmid with changes accommodating the request of the synthesizing company.....	27
Figure 12. Newly emerged bees GCMS sugar quantification.....	30
Figure 13. Nurse bees GCMS sugar quantification.....	31
Figure 14. Forager bees GCMS sugar quantification.....	31
Figure 15 qPCR of Forager bees using ILP-1 and ILP-2.	32
Figure 16 Live cell imaging of Fura-2 dyed Ame711 cells.....	33
Figure 17 Ratio of the signals obtain from Fura-2AM (340/380nm).....	33
Figure S1. ILP1 Primer validation gel electrophoresis.....	51
Figure S2. Chromatogram from GCMS.....	51
Figure S3. Showing the cells loaded with Fura-2.....	52
Figure S4. Network created using BioGRID that shows the interactions between CAMKII and OAMB.....	53
Figure S5. The biogenic amine levels on a per brain basis of Octopamine across newly emerged (blue), nurse (red), and forager bees (green).....	54

Figure S6 (A) Octopamine 1mM (agonist) was added to the cells at 1.5mins. Replicate #1.....55

Figure S6 (B) Octopamine 7mM (agonist) was added to the cells at 1.5mins. Replicate #2.....55

Figure S6 (C) Octopamine 7mM (agonist) was added to the cells at 1.5mins. Replicate #3.....56

Figure S6 (D) Octopamine 7mM (agonist) was added to the cells at 1.5mins. Replicate #4.....56

Figure S6 (E) Octopamine 7mM (agonist) was added to the cells at 1.5mins. Replicate #5.....57

LIST OF ABBREVIATIONS

AAV	Adeno-Associated virus
AmOct β 2	Apis mellifera Octopamine receptor beta subtype 2
BSTFA	N,O-Bistrifluoroacetamide
DNA	Deoxyribonucleic acid
Cas	CRISPR-associated protein 9
CRISPR	Clustered repeating interspaced palindromic repeats
GCMS	Gas chromatography- Mass spectrometry
GFP	Green fluorescent protein
HDR	Homology directed repair
HPLC	High pressure liquid chromatography
NHEJ	Non-Homologous end joining
OA	Octopamine
OAMB	Octopamine receptor in mushroom bodies
PAM	Protospacer adjacent motif
PER	Proboscis extension response
RNA	Ribonucleic acid
Sf9	Spodoptera frugiperda

1. INTRODUCTION

1.1 General overview

The most recent decline in health can be attributed mainly to parasites, pesticide exposure, and loss of foraging habitat. All of these factors can act in concert, resulting in energetic stress for the honeybee. The honey bee health decline is putting the world food supply at a great risk, because without the honey bee, agricultural plants requiring pollination would also decline in number (van der Sluijs & Vaage, 2016). All organisms face the challenge of maintaining energetic homeostasis, and as a result there is a constant selection pressure to optimize this, but how this is accomplished in many organisms remains yet to be elucidated (S. Nelson Thompson, 2003)). An integral part of maintaining energetic homeostasis stems from the regulation of appetite, which is also known as the likelihood of feeding or the potential to ingest food (Simpson & Raubenheimer, 1993). This is different from hunger which reflects the physiological demand for energy or food, directly reflecting the organism's energetic state (Zhao, Chi, Cao, & Han, 2010).

There are three main sugars found in insect hemolymph (blood), which are glucose, fructose, and trehalose. However, in insect's trehalose, instead of glucose, is the primary sugar found in the hemolymph (Q. W. Chan, Howes, & Foster, 2006; Woodring, Boulden, Das, & Gäde, 1993). Due to the open circulatory system found in insects, hemolymph is constantly circulating around the body to deliver nutrients and carry away waste (Miller, 1997). Hence, the contents within hemolymph can be the best indicators of the organism's energetic state,

and the sugar levels, in particular trehalose levels, are constantly fluctuating (S.N. Thompson, 2003), reflecting the energy reserves available, in real time, that the organism can use to carry out life activities (Wang, Brent, Fennern, & Amdam, 2012).

The honey bee, in particular the forager honey bee, is an excellent model organism to investigate appetite regulation. When a honey bee is foraging, the energetic demand increases greatly in order to sustain flight, but during this activity some time is also spent in the hive where there are ample food stores and little activity is needed (Korst & Velthuis, 1982). Therefore, the energetic demands of a forager bee are constantly changing, requiring precise appetite regulation, in order to maintain energetic homeostasis. This study attempts to provide new insights into the neurological and physiological mechanisms involved in the maintenance of energetic homeostasis. We study this across the bee as it ages because the energetic demand varies drastically based on age-dependent activities carried out by the honey bee throughout its lifetime (J. M. Harrison, 1986). More specifically, we aim to determine if there is a cause-and-effect relationship between fluctuating hemolymph trehalose levels and octopamine levels in the brain, which results in appetite regulation independent of the glucose-insulin signaling pathway. In order to accomplish this, a custom CRISPR-Cas9 system has been designed to specifically target and knockdown the octopamine beta receptor subtype 2 in the bee brain to study its involvement in appetite regulation. The beta receptor was chosen over the alpha because, the effects of the alpha subtype are better understood, it is known to play a role in appetitive olfactory learning and memory pathways and is located in the antennal lobe region of the honey bee brain (Farooqui et al. 2004). The beta receptor subtype 2 is the has the most abundant gene expression in the bee brain, so this was chosen over the other three as a starting point to determine if the beta receptors play a role in appetite regulation.

1.2 Trehalose in relation to appetite

Trehalose is a sugar composed of two glucose subunits and has been reported to be the sole sugar responsible for honey bee crop emptying rates. This supports the notion that variation in the trehalose levels in the hemolymph may serve as an indicator of the honey bee's energetic state (Roces & Blatt, 1999a). Trehalose is also known to be the source of energy to fuel flight

for foraging honey bees, as it is broken down into glucose, to maintain steady levels of this sugar and to power the flight muscles (Jasmina Blatt & Roces, 2001a). When glucose levels are too high, they are converted to trehalose by the trehalase p-synthase enzyme. Therefore, glucose levels are maintained at a relatively constant level at the expense of trehalose. Consequently, it has been proposed that out of the three sugars, trehalose with its fluctuating levels, is the key sugar used to monitor the energetic state of the honey bee (S.N. Thompson, 2003).

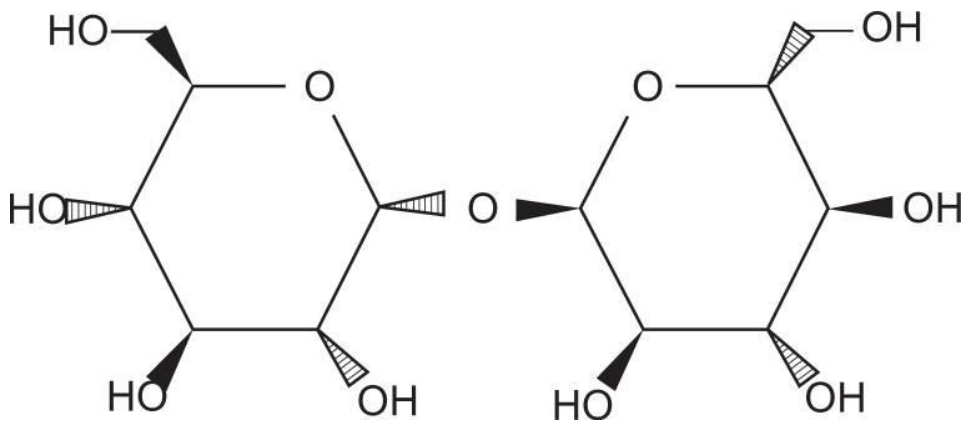


Figure 1. Trehalose which is composed of two glucose molecules bound together (Luyckx & Baudouin, 2011).

1.3 Octopamine receptors in the honey bee brain

Octopamine (OA) is one of four biogenic amines found in insects, it can act as a hormone, neurohormone, or neurotransmitter. OA is analogous to norepinephrine in vertebrates so the levels are much higher in invertebrates than in vertebrates because vertebrates lack octopamine receptors (Axelrod & Saavedra, 1977). It has been reported that foragers exhibit increased levels of OA in response to starvation, the energetic demand of an organism (Mayack et al., 2019). Furthermore, it has been reported that increased appetite, the potential to feed, also correlates with increased levels of OA (Scheiner, Plückerhahn, Oney, Blenau, & Erber, 2002). In addition, OA levels have been reported to be linked with feeding behavioral responses in

Drosophila melanogaster (Youn, Kirkhart, Chia, & Scott, 2018). More crucially, in this study it is shown that due to the decreasing levels of OA, there is a resulting decrease in appetite as well. Therefore, we suspect that in the honey bee there is a connection between the fluctuating trehalose in the hemolymph, and octopamine levels in the brain that results in appetite regulation. In the honey bee, octopamine binds to both octopamine alpha (Grohmann et al., 2003) and beta receptors. These receptors are part of the G protein-coupled receptors, that include, 2 alpha subtypes and 4 beta subtypes (Blenau, Wilms, Balfanz, & Baumann, 2020). At the molecular level, the alpha subtype 1 results in a calcium signaling cascade, while the subtype 2 results in a regulation of cAMP. Beta subtypes are lesser studied, but proposed to also have an effect on cAMP activity.

We aim to knockdown the newly characterized octopamine beta receptor subtypes to determine which one plays a role in appetite regulation. CRISPR-Cas9 will be used for the knockdown of the different octopamine beta receptor subtypes 2. To date, the transgenic tools remain limited for the honey bee, and optimal *in vivo* vectoring methods remain largely unknown (Ikeda et al., 2011). Plasmid introduction of promoters using electroporation to manipulate gene expression for different gene targets have proved to have limited penetration into the central processing regions of the brain such as the mushroom body (Schulte et al., 2013). Furthermore, the lentivirus used for vectoring the CRISPR-cas9 complex for mammalian cells has shown low transduction efficiency of around 20% for honey bee cells (M. M. Chan et al., 2010). We, therefore, instead propose to use a baculovirus vector for the CRISPR-cas9 complex because it is known to have a high infectivity rate for insect cells, which could lead to higher transduction efficiencies (Kost, Condreay, & Jarvis, 2005).

Previously the baculovirus vector has been used successfully for manipulating the expression of G-protein coupled receptors (Gazi, Nickolls, & Strange, 2003; Massotte, 2003). Deformed wing virus, for example, is known to infect the brain of the honey bee (Shah, Evans, & Pizzorno, 2009) so we hypothesize that a virus would be the best way to vector the CRISPR-cas9 complex over other methods such as gold nanoparticles and lipo-vesicles, which rely only on diffusion for them to reach the tissue target and not production of the CRISPR-Cas9 system from the organism (Horodecka & Döchler, 2021). First, we will determine its transduction

efficiency using the honey bee cell line *in vitro* and compare this to lentivirus performance. Then, we will inject the baculovirus into the honey bee brain to obtain our desired effect of knocking down the octopamine beta receptor subtype 2 because this receptor is most commonly expressed in the honeybee brain, but also is located in other parts of the honey bee body so a localized injection is most likely to give the desired effect (Balfanz et al., 2014). Once this methodology is established, it can be used as a model for the other honey bee octopamine beta receptor subtypes to determine their role in appetite regulation. From this knockdown, we predict a lowering of appetite levels if octopamine is indeed playing a role in appetite regulation of the honey bee because less receptors will be functional for octopamine signaling.

1.4 CRISPR-Cas9

Clustered regularly interspaced short palindromic repeats, CRISPR, combines with the CRISPR-associated protein 9 (Cas9) to provide a powerful gene-editing tool that has revolutionized genetic studies and therapies. The CRISPR-Cas9 system was initially observed as part of the adaptive immune system of bacteria, in which there was an RNA guided nuclease (Cas). This mechanism enables the bacterium to identify and breakdown exogenous sequences of viral origin. Furthermore, it was observed that parts of the exogenous genetic information were integrated into the bacterial genome, which would go on to serve as a memory of past invaders (Thurtle-Schmidt & Lo, 2018).

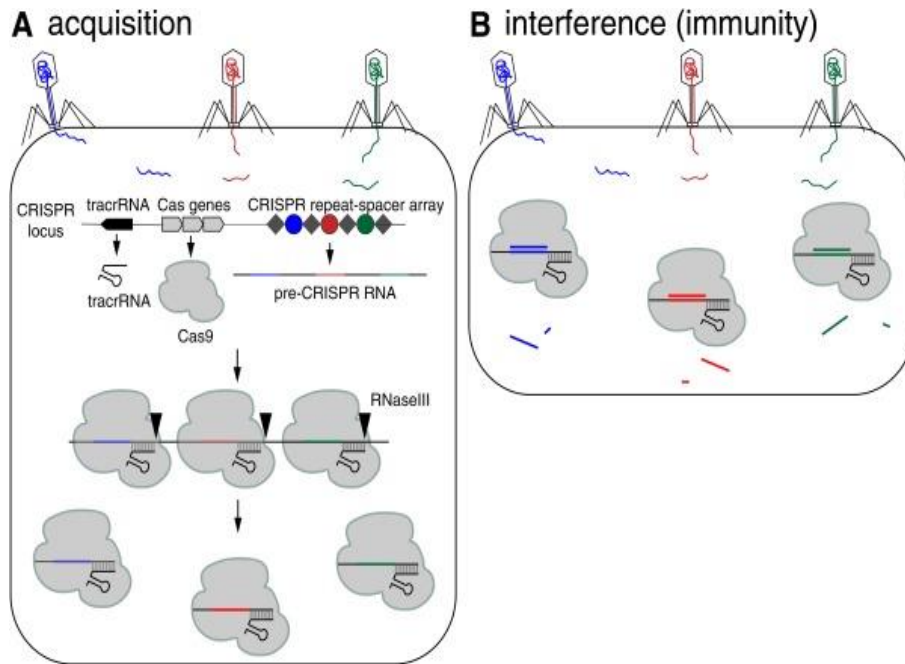


Figure 2. CRISPR Cas9 discovery, the mechanism behind bacterial immunity. (A) A schematic indicating how the bacteria obtained the foreign sequences of DNA, and how they are incorporated into the bacteria's DNA and then into Cas9. (B) This image shows how the Cas9 is being used by bacteria to act as a form of immunity.

The integrated DNA is separated by repeat sequences (Grey), the spacers (colored, integrated), upon transcription code for the spacer sequences, as can be seen in **Figure 2**. The pre-CRISPR RNA gets cleaved to give rise to crRNAs, which associate with Cas proteins. The crRNAs serve as guides that upon the detection of complementary sequences result in their fragmentation; this can be observed in part B of **Figure 2**.

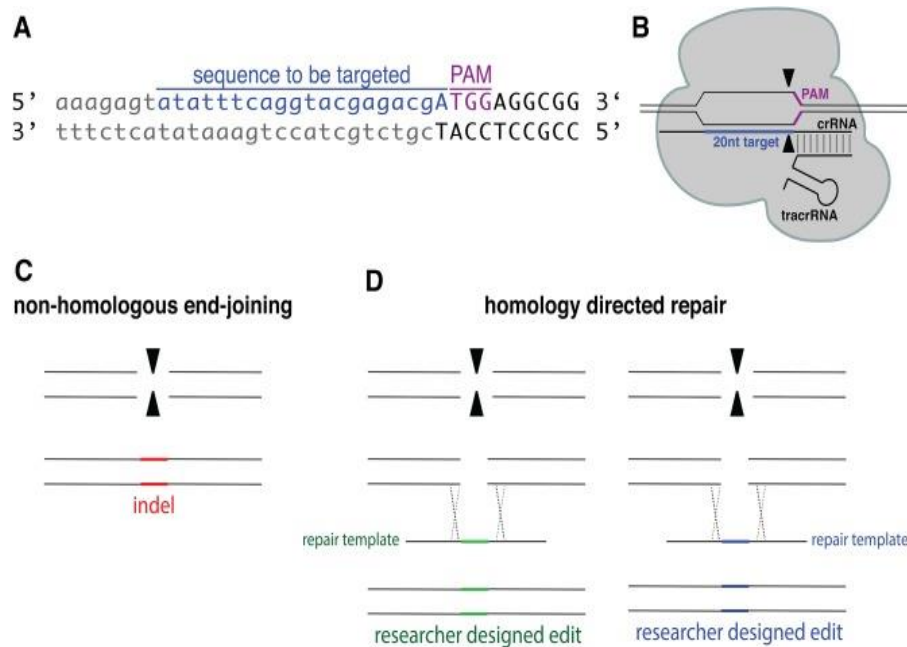


Figure 3. The various approaches that the Cas9 enzyme may be used to create various genetic edits (A) Showing the location of the target sequence, which is paired with PAM sequence. (B) The parts of the designed sequence to be targeted and where it attaches, where the double stranded break will be made, and where this is relative to other sequences. (C) Depicts NHEJ, non-homologous end-joining that occurs after the DNA break is made. (D) Depicts homology direct repair in which a gene of interest is inserted where the cut in the DNA is made (Thurtle-Schmidt & Lo, 2018).

There are two ways in which the CRISPR-Cas9 complex can be used for gene editing. One way is from repairing non homologous end joining (NHEJ) and the other is via homology directed repair (HDR). With HDR, base pair modifications, as dictated by the researchers, are included in the repair template, which go on to being integrated by the cell repair mechanisms. On the other hand, with NHEJ errors are made during the repair, and in most cases, rendering its corresponding protein non-functional. In this work, we aim to use the NHEJ process for octopamine beta receptor subtype 2 knockdown. Lastly, it should be noted that a PAM (Protospacer Adjacent Motif) sequence is required to be upstream or downstream of the sequence to be targeted (dictated by the gRNA). The variation of the PAM sequence is based on the Cas protein used. PAM doesn't code for anything specific, but instead has been shown to aid the Cas protein in locating exactly where the DNA cut site will be, the location of this cut is indicated by the black arrows in **Figure 3**. This PAM sequence can be obtained from

previous studies or be designed *in silico* using algorithms such as CHOP-CHOP, flyCRISPR, and Benchling.

There are many ways by which CRISPR/Cas9 components may be introduced into the desired cell. One way is to introduce them is by the utilization of plasmids coding for Cas9 protein and the crRNA, as seen in **Figure 3A**, this entire plasmid can then be inserted into a virus, and the virus serves as a vector for producing the CRISPR-cas9 complex from the host cell. Other methods include the direct introduction (via microinjection for instance) of previously synthesized gRNA (B) and/or the Cas protein (C). Although it is significantly easier to directly inject the Cas9 protein or Cas9 plasmid into the cells, it is quite time consuming, as it requires a cell to be injected one by one. Furthermore, this approach requires a costly microinjector setup, which may not be accessible. Furthermore, once the Cas9 protein is consumed, it must be produced and re-introduced once again. However, with the use of viral vectors, more can be easily generated both in the lab and by the host cell itself. More of the plasmids can be generated using *E. coli* cultures, and more viruses can be made using a dedicated cell line where they are infected to continue to propagate the virus for future use, a common one used for this purpose is the Sf9 cell line. Potential downsides are the fact that not all viral vectors are easily used as some are infectious to humans, while others have a limit on how big a plasmid can be packaged by the virus.

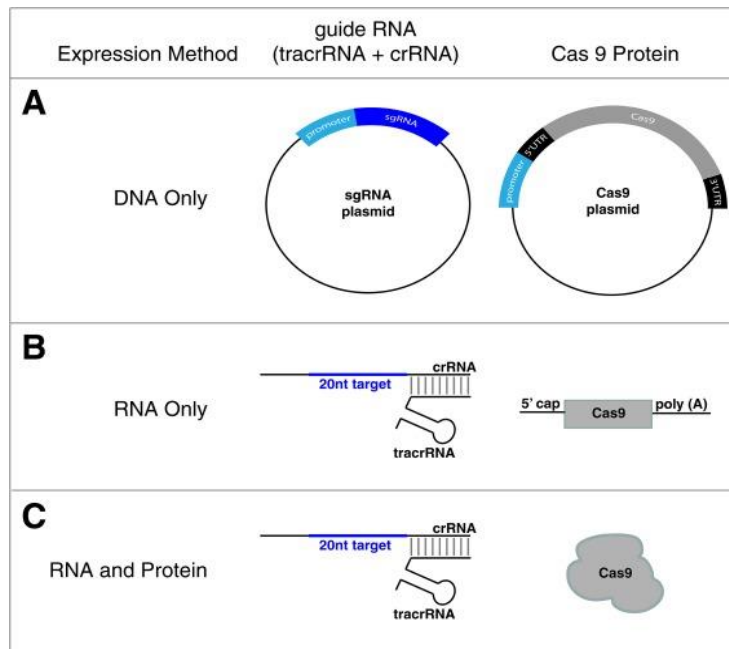


Figure 4. Depiction of various ways that Cas9 and gRNA could be introduced into cells. Grouped up by the expression method. (A) The introduction of Cas9 and gRNA using plasmids. (B) The introduction of gRNA and Cas9 via RNA (C) The introduction of the cas9 protein directly, as well as the gRNA directly (Thurtle-Schmidt & Lo, 2018).

Research carried out on the only *Apis mellifera* cell line, Ame711, is quite rare, if not non-existent in the literature. Baculovirus vectors were previously utilized in honey bee queens with success (Ikeda et al., 2011). In general, baculoviruses are known to have higher transduction efficiency in insects in comparison to lentiviruses and Adeno-associated viruses (AAV) (Kalesnykas et al., 2017). Furthermore, baculoviruses, when compared with other viruses, present a lower biological health hazard to humans (Stacey & Possee, 1996). Honey bee cell lines were not available commercially at the time of this study, hence honey bee cells were obtained directly from Dr. Michael Goblirsch, the original creator of this line. This cell line, Ame711, was generated from primary cells originated from eggs in late embryogenesis stages (Goblirsch, Spivak, & Kurti, 2013). Here, we propose first testing the transduction efficiency of the baculovirus on the honey bee cell line to verify its efficacy using GFP before conducting *in vivo* injections into the honey bee brain to evaluate its effect on appetite regulation.

1.5 Cell lines

Cell lines have been in use now for over 100 years, from with the first ever cell line used to study frog nerve cells (R. G. Harrison, 1906), to the first ever immortal human cell line, HeLa cells (Eagle, 1955). In respect to insect cell lines, the most commonly used include: the S2 cell line (*Drosophila melanogaster*), the Sf9 cell line, (*Spodoptera frugiperda*), and the Ame-711 cell line (*Apis mellifera*). This cell line was originally created using honey bee embryos.

Because the honey bee cell lines are not available commercially, and hence are quite rare, we aimed to further characterize it to determine if the cells contain the octopamine subtype 2 beta receptor.

One way to confirm if there is octopamine receptor activity within the cell line is to measure calcium signaling using the biosensor, Fura-2. Essentially, this is a ratiometric stain that binds to the Ca^{2+} that is free floating intracellularly. Fura-2 is excited at both 340 nm and 380 nm (Grynkiewicz, Poenie, & Tsien, 1985). The ratio of these two excitation wavelengths (340/380) is proportional to the amounts of intracellular Ca^{2+} . The main benefit in relation to our research objectives is to show that the cell line contains octopamine receptors that are functioning in real-time. Another benefit from using Fura-2 to stain the cells is that it paves the way for future signaling research on the cell line. This is arguably a monumental step toward the widespread use of this cell line. This is because no honey bee cell lines exist commercially, or are widespread among the scientific community. Providing evidence that these cells “talk” using calcium, would allow for research to be carried out on honey bees *in vitro*, instead of only being limited by *in vivo* studies.

2. AIM OF THE STUDY

This study has two main aims, the first one focuses on testing whether fluctuating levels of trehalose in the honey bee hemolymph result in a variation of OA levels in the bee brain and consequently appetite levels.

In parallel with the first aim, we will confirm whether OA is the causal link between fluctuating hemolymph trehalose levels and appetite regulation. This aim will be tested by creating a knockdown of the *Apis mellifera* beta subtype 2 octopamine receptor (AmOct β 2) in the honey bee brain. The knockdown will be carried out using a CRISPR/cas9 system. The CRISPR-cas9 system will first be verified, and its vectoring system will be optimized *in vitro* using a honey bee cell line. Then the CRISPR-cas9 system will be used *in vivo* for the knockdown of the octopamine beta receptor subtype 2 in the bee brain to determine its role in appetite regulation.

3. MATERIALS & METHODS

3.1 Materials

3.1.1 Chemicals

All the chemicals that were used in this project can be found in Appendix A.

3.1.2 Equipment

All the equipment that was used in this project can be found in Appendix B.

3.1.3 Molecular biology Kits

All of the kits that were used in this project can be found in Appendix C.

3.1.4 Software, websites, and computer-based applications

The list of software, websites, and computer-based applications can be found in the table below.

Table 3.1. List of software, websites, and computer-based applications

Software, website, Application name	COMPANY/WEBSITE	PURPOSE
NCBI	https://blast.ncbi.nlm.nih.gov/Blast.cgi	Alignment tool
Addgene	https://www.addgene.org/	Plasmid repository

Snappgene	Snappgene	Plasmid construction and viewing
Benchling	https://www.benchling.com/	PAM sequence generation and analysis
Biogrid	https://thebiogrid.org/	Pathway mapping
R studio	R-Tools	Statistical tests on data was carried out using R
GCMS Realtime analysis	Shimadzu	Real time view of chromatographs as they are generated, setting the GCMS instrument parameters
GCMS postrun analysis	Shimadzu	Analysis of Chromatographs generated by the GCMS
Zeiss Zen software	Zeiss	Capturing and analyzing Fura-2 staining images

3.2 Methods

3.2.1 Collection, marking and injection of the bees with different sugars

All age groups of bees were targeted for injection, this includes: Newly emerged, nurse bees and forager bees. First a brood frame was taken out of a healthy hive; any other bees present on this frame were removed. This frame was then placed into a metal enclosure that was placed inside a humid incubator at 32°C and 70% relative humidity. The frame was checked daily, and any bees that emerged within 24 hr. were paint-marked using Testors enamel paint on the back of their thorax and then sprayed with scented 30% sucrose solution, to be released back into the hive. The newly emerged bees were immediately used for experiments, while the marked bees were recaptured about 7 d later and these were considered to be nurse bees. Marked bees recaptured about 4 weeks after reintroduction were considered to be forager bees. The bees were divided into groups and injected with 1 µl of one of the following 5 different sugars: fucose (3 M), fructose (3 M), trehalose (1.5 M), sorbose (10% w/v), and glucose (3 M). Furthermore, the control group, was injected with 1 µl of Ringer's solution.

In order to maintain consistent injection conditions, the bees were harnessed in the laboratory by placing them inside a straw with a piece of 1 mm wide duct tape strip between the thorax and head that wrapped around the front of the bee and secured on the outside of the straw. The bees were injected into their thorax with each respective sugar per treatment group using a 10 µl Hamilton syringe. In the first experiment, 15 min after the injection, the appetite of the bee was measured using the Proboscis Extension Response (PER) assay. This involved touching the bee's antennae with a droplet of sucrose solution without allowing them to feed on it and recording whether or not the bee extended its proboscis in an attempt to feed on the droplet of sucrose solution. Each individual bee was tested using increasing concentrations of sucrose solution as follows: 0%, 0.1%, 0.3%, 1%, 3%, 10%, and 30%. In between each assay, a droplet of water was touched to the bee's antennae to prevent desensitization (Bitterman, Menzel, Fietz, & Schäfer, 1983). After this the hemolymph of each bee was extracted from the abdomen using a 1 µl Drummond glass microcapillary. The hemolymph was extracted by pricking the bee in between the second and third abdominal segment using an insect pin. The bees were then stored at -80° C until IPL1-2 qPCR analysis.

In the second experiment, only forager bees were subjected to 1 μ l thorax injections of trehalose (1.5 M) and 10% sorbose along with ringer's solution that also acted as a control. In preparation for storing and dry ice dissections of the brains, the bees were flash frozen in liquid nitrogen, then their heads were removed and placed in labelled 1.5 ml microcentrifuge tubes. These were then stored at -80° C until HPLC biogenic amine analysis.

3.2.3. Quantification of sugars in hemolymph using GC-MS

3.2.3.1. Sample preparation & lyophilization

For external standards, 10 mg/mL stocks of glucose, fructose, trehalose and fucose were prepared by measuring 20 mg of each sugar and dissolving it in 2 ml of Millipore water. The external standards were then prepared by pipetting the volumes indicated in **Table. 1** from the stock solution in to water, the final volume was 1 ml.

Table 3.2 Volumes of each sugar to be added to the external standard stocks.

<i>Sugar</i>	A	B	C	D	E	F
<i>Glucose</i>	0.167	3.333	6.667	10.000	13.333	16.667
<i>Fructose</i>	16.667	13.333	10.000	6.667	3.333	0.167
<i>Trehalose</i>	3.333	0.167	6.667	10.000	13.333	16.667
<i>Fucose</i>	10.000	16.667	0.167	3.333	13.333	6.667
Total:	30.167	33.500	23.500	30.000	43.333	40.167
<i>Water</i>	969.833	966.500	976.500	970.000	956.667	959.833

Previously extracted hemolymph samples were diluted 1:1000 with autoclaved Millipore water. For a 1:300 dilution, 33.3 μ l of each sample was aliquoted to separate 1.5 ml microcentrifuge tube. These tubes were then covered with a Parafilm layer with pin pricked

holes created using an insect pin. In addition, 10 μ l of each external standard was added to a separate 1.5 ml tube, that was also covered in Parafilm with holes created using an insect pin. Both sets of tubes, external standards, as well as the samples containing tubes were lyophilized using the Freeze Dryer TRS 2-2V, overnight, for the removal of all water content.

3.2.3.2 Derivatization

For detection via GC-MS, the sugars had to be derivatized. This was carried out by adding 10 μ l pyridine with 1.25 mg/ml hexachlorobenzene as the internal standard to the respective 1.5 mL tubes. Furthermore, 20 μ l of N,O-Bistrifluoroacetamide (BSTFA) 1% Trimethylchlorosilane (TCMS) (Thermoscientific) was also added to each tube; the tube was immediately closed to avoid contact with humidity in the air. Each tube was then vortexed for 30 s. The top of each tube was covered with parafilm to minimize evaporation. The tubes were then heated at 70° C for 3 h using a heat block. The tubes were then placed on a tabletop mini centrifuge and spun for 15 s. As the tube cools, any vapors would condense to the bottom of the tube while being spun. The samples and external standards were then transferred to 100 μ l glass inserts, that were inside 2 ml glass amber micro vials. This was done in a quick fashion in order to reduce the time the samples spent in contact with the air, as humidity in the air tends to rapidly reverse the derivatization reaction that was carried out.

3.2.3.3 GC-MS analysis

The hemolymph samples as well as the external standards were analyzed using a Shimadzu QP-2010 ULTRA GC-MS. The carrier gas used was helium, with a flowrate of 1.3 ml/min. We used a Restek column Rtx-5MS, length 60 m, thickness 0.25 μ m, diameter 0.25 μ m. The temperature of the injector was set to 280° C, and the mass spectrometer inlet

temperature was set to 230° C. Furthermore, the injection temperature was set to 65° C, held for 2 min, increased by 6° C per min, to finally reach 300° C, which was held for 15 min. In addition, the mass spectrometer, MS, was set to electron ionization mode.

Upon running the derivatized standards, their respective peaks were identified by comparing the retention times of the external standards and the m/z numbers based on the ones reported in PubChem. The sugars' identities were further confirmed by using a similarity search, where the hits that had had a similarity score above 80% were expected to be the target compound. Initial readings are presented in the chromatogram Figure S2, where each of the corresponding peaks is labelled. The peaks of the target sugars (trehalose, fructose, fucose, and glucose) were manually integrated and then normalized via the internal standard peak area. The external standard mixture was run such that in total there was 6 different concentration levels per sugar, as can be seen in **Table 1**. These standards were used to form the standard calibration curves for the quantification of each sugar in mg/ml.

3.2.1.1 Dissections

The bees were stored at – 80°C in order to preserve the biogenic amines present in their brain tissues. The brains were dissected on dry ice using a dissecting scope and a microfeather micro scalpel. Each dissection started by the removal of the chitin layer. **Figure 5a** shows the head upon removal of the chitin layer. Then the optical lobes and the hypopharyngeal glands were removed in that respective order as shown in **Figure 5b**. The brain was then placed in a 1.5 ml microcentrifuge tube and stored at -80°C until further HPLC analysis was carried out.

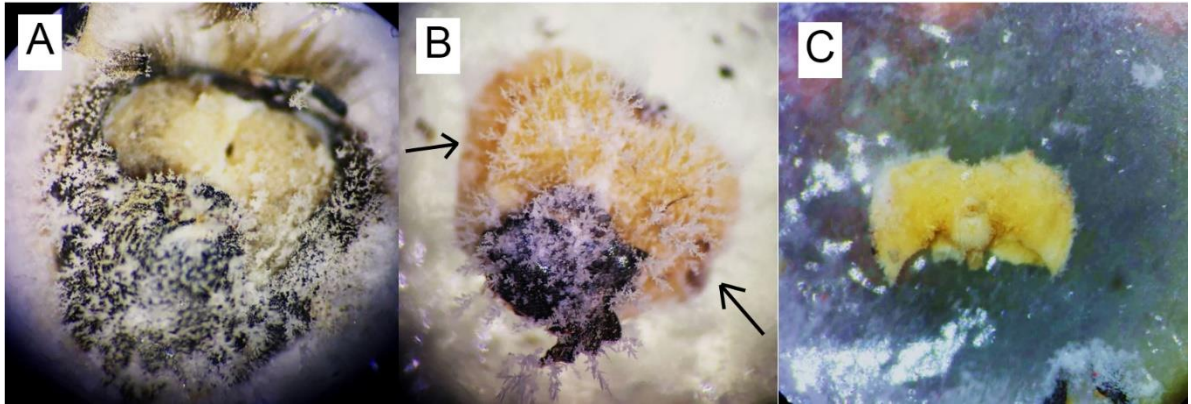


Figure 5. Honey bee brain dissections on dry ice. Three pictures taken at different stages of brain dissections. (A) A bee head upon the removal of some of the chitin layer, (B) a bee brain after most of the chitin layer has been removed with the optical lobes indicated with black arrows, and (C) a completely intact brain at the end of the dissection, after removal of the optical lobes.

3.2.4 qPCR gene expression analysis of ILP1-2

The treated bees, thorax and abdomen, were obtained and placed in 1.5 ml micro centrifuge tubes. Then they were macerated using a sterile pestle while submerged in 1 ml of One step RNA reagent (BS410A, BIO BASIC, Markham ON, Canada). The RNA was then isolated as per the kits' manufacturer's instructions. Then the RNA was purified by using EZ-10 spin Column Total RNA Minipreps Super Kit (BS784, BIO BASIC, Markham ON, Canada) as per the kits' manufacturer's instructions. The purity and concentration of the extracted RNA was measured for each sample using a Nanodrop spectrophotometer. The cDNA was then synthesized according the manufacturer's instructions by using the OneScript cDNA Synthesis Kit (AccuRT Genomic DNA Removal Kit, location). Then, in each well of a 96 well plate (Axygen PCR MICROPLATE), the following was added: 5 μ l of green nucleic acid dye (Abm Blastaq Green 2x PCR, Richmond BC, Canada), 1.2 μ l of forward and reverse of either ILP1 or ILP2 primer (SenteBioLab, Ankara, Turkey), 2.8 μ l of water (WISENT Multicell Sterile water, nuclease free water), and 1 μ l of template cDNA. The thermocycler (Roche LightCycler 480 II) parameters on the software were set to quantification for 50 cycles (95°C, 30 sec ramp rate 2.2, 60°C ramp rate 2.2, 30 s, 72°C ramp rate 4.4, 1 min).

3.2.5 CRISPR-cas9 knockdowns of octopamine receptors in the bee brain

3.2.5.1. Cell culturing and characterization of the cell line

This cell line was originally created by obtaining honey bee eggs and crushing them to release the embryos using a pestle. The embryonic cells were then cultured using HB-1 medium (Goblirsch et al., 2013). However, upon further testing by Goblirsch et al., (2013), it was found that the cells grow in a healthy manner using Schneider's insect medium. We were advised to add 20% of heat inactivated FBS to aliquots of the medium, but we found that the cells were even healthier when 10% FBS was used. We found that in its healthiest state, the cells were ready to split on average within 7 days.

The stock culture was maintained in a 25 cm³ flask with Schneider's insect medium (Sigma Aldrich), after adding 10% heat activated FBS. We placed the flask in a sterile incubator set to 32° C. Compared to other more established cell lines, Ame711 exhibited a substantially slower splitting time, which was 5 - 10 d. When the cell cultures exhibited 80% confluency or in some cases even higher, Goblirsch et al. (2013) had noted that the cells' growth was limited by contact, and this is something we have also observed, as can be seen in **Figure 6B**, so at the confluency percentage of >80% they were split into a 1:2 ratio. This was done by first removing the medium from the surface and then adding 1 ml of trypsin and placing the flask at 32°C for 3 min. The cells were then dislodged by delivering a blow to the side of the flask. Trypsinization was then halted by adding 1 ml of fresh medium. Finally, to ensure most cells detach from the flask, they were gently scraped off the bottom of the flask using a cell scraper (99002, 240mm, TPP, Switzerland). It is important to note that Schneider's medium tends to crystallize due to precipitation and in the presence of salts so periodic replenishment of the medium was carried out, typically every 5 d.

Antibiotics may interfere with transfection; therefore, the cell line was maintained in two different conditions, one with antibiotics and one without. The antibiotics used were penicillin-streptomycin-Amphotericin (0.1%), and noromycin (0.1%). The cell line was continuously maintained throughout the duration of the *in vitro* experiments so that cells were readily available to evaluate the transduction efficiency of the baculovirus.

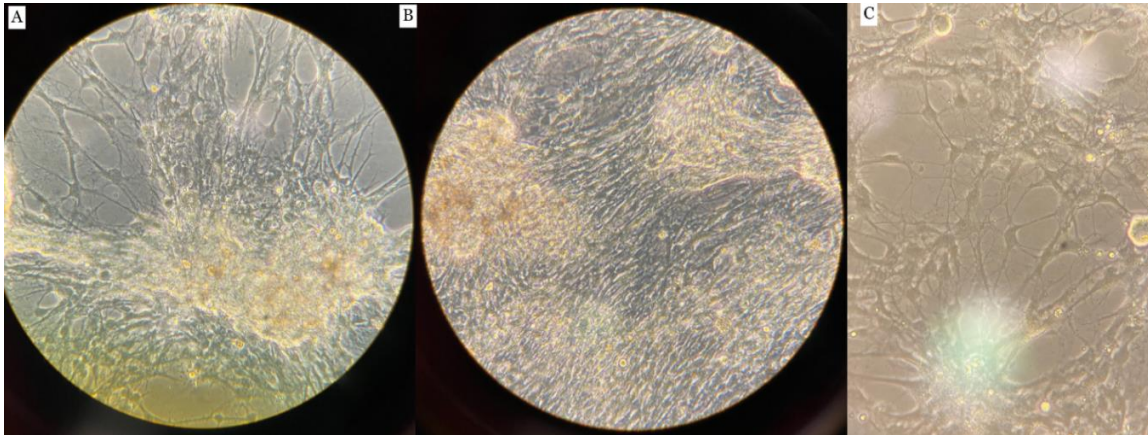


Figure 6. Light microscope images of the Ame711 cell line, with 40X zoom. (A) A microscope image showing the cells from the honey bee cell line and how they aggregate towards localized clusters. The darkened lines and round shapes indicate the individual cells. (B) This image shows the cells at a 100% confluency. (C) This is a digital close of up the cells showing how they interact with other cells.

3.2.5.2 Calcium cell imaging

Upon reaching > 80% confluency, the medium was discarded from the flask. The cells were treated with trypsin (0.05% Trypsin, Multicell, Wisent, Canada), and set to incubate for 5 min at 32° C, after which a blow was delivered to the side of the flask. A total of 6 ml of Schneider's insect medium supplemented with 10% FBS was added to the flask. The cells were then fully dislodged using a cell scraper (30cm, TPP, Switzerland). The contents of the flask were then transferred to a 15 ml falcon tube, medium was added to bring up the volume to 12 ml, and gentle pipetting was used to reduce the number of clumped cells. A total of 2 ml of cells suspended in medium were added to each well in a 6 well plate (CellStar, Greiner Bio-One). The 6 well plate contained 30 mm round cover slips that will be used for imaging. These cover slips were treated with 1% w/v poly-l-lysine (Sigma,

Germany) (as much as needed to submerge the cover slips, about 2 – 3 ml) for 24 h in order to promote cell adhesion to the cover slips. The cells were left overnight to allow them to fully attach to the cover slips. Furthermore, the cells were treated with a physiological salt solution that serves to supplement the cells with the required calcium ions that will be visualized. This solution was prepared according to previous literature (Millar et al., 1995); the detailed contents can be found in the table below. In addition, octopamine was added to a separate 15 ml falcon tube, and then diluted such that the final concentration was 7 mM, finally Fura-2 was added at a concentration of 3.3 mM. The medium was discarded off the cells and then they are washed with the physiological solution twice. Then 1 mL the second solution, containing Fura-2 and octopamine, was added to each well. This was then covered with aluminum foil and left to incubate for 30 min. Each well was then washed again with 1 ml of physiological solution. Again, Fura-2 containing solution was added and the 6 well plate was left to incubate for 50 min at room temperature covered in aluminum foil to prevent photobleaching of Fura-2. Each cover slip was then removed using fine tweezers and placed inside the imaging chamber, which was then secured to the microscope and attached two lines of physiological solution, one without octopamine, so that switching between each line allowed for the addition of octopamine. The imaging chamber was then placed under a Zeiss fluorescence microscope using a 20x objective lens.

Table 3.3 Composition of the calcium containing physiological solution

Components	Concentration (mM)	1000ml total
CaCl₂	2	20 ml of 0.1 M
NaCl	120	120 ml of 0.1 M
MgCl₂	8	8 ml of 0.1 M
KCl	5	50 ml of 0.1 M
Hepes	10	10 of 1.0 M
Sucrose	32	11 g
pH (NaOH)	7.2	~3-5 ml of 1.0 M

3.2.5.3. Plasmid design

Phase I

In this project, the CRISPR-Cas9 system will be introduced into the Ame-711 cells via baculovirus, more specifically the *Autographa californica nucleopolyhedrovirus* (AcNPV). The initially proposed plasmid designs can be seen in **Figure 7**. Construct B was designed such that basic infectivity can be tested because this is the first time that this specific cell line will be infected with baculovirus. Consequently a simple plasmid containing ACGFP1 was designed to allow for visualization of GFP fluorescence, and potential quantification later on of the infected cells to determine the transduction efficiency of the virus *in vitro*, by comparing the ratio of GFP fluorescing cells to the non-fluorescent cells. This quantification can be achieved via obtaining images of the cells via fluorescence microscopy and then counting the transduced cells to obtain a percentage of infected cells. In addition, the PAC gene, (puromycin N-acetyltransferase) was also included in order to provide a selection mechanism. If a cell has been correctly transduced, then it should exhibit resistance from the PAC gene, and hence, it would survive in an environment that has puromycin in it. Furthermore, based on the previous literature that (A) also using baculovirus for transduction of *Apis mellifera* queen bees, the Pcmv gene (B) led to the constructs as it is the cytomegalovirus immediate-early gene promoter (Ikeda et al., 2011). Towards the end of this first iteration of the plasmid, only the overall layout was present, without even sequences.

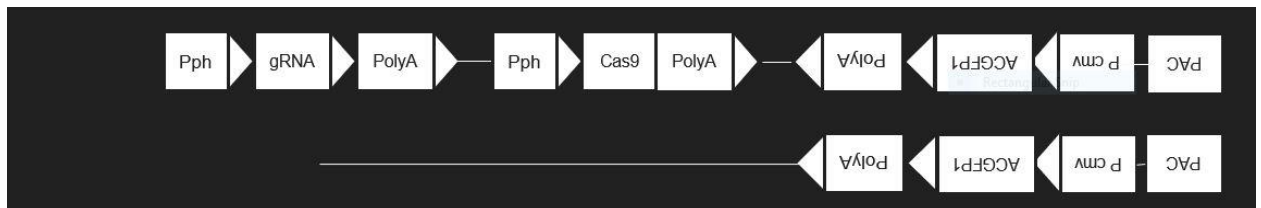


Figure 7. Initial proposed plasmid constructs A and B. This diagram shows the layout of the first two proposed designs of the plasmid. Construct A was proposed such that gRNA and Cas9 could be delivered, within the same construct, GFP was also going to be used as an indicator for a successful knockdown. Construct B would be used to test whether or not we could simply insert GFP into the cells and have it expressed using the promoters as labelled.

Phase II

During the second phase of plasmid design, it was decided that a backbone plasmid was going to be used as a starting point. However, since there was little to no transductions of any kind (via baculovirus or otherwise) being carried out on honey bees, previously designed plasmids were rare. Therefore, we relied on *Drosophila melanogaster*, commonly known as the fruit fly, to be used as a template. Hence, the starting plasmid that was obtained from Addgene, was initially intended for use on the fruit fly (Bassett, Tibbit, Ponting, & Liu, 2014). The first step that was taken was to find a promoter that is highly expressed and consistently in honey bees under a number of conditions. Previous reporting documented and tested the expression levels of a honey bee ortholog of Actin5c, which was expressed under different conditions, this was called Am-actin5c (Schulte et al., 2013). Nevertheless, the sequence provided by that article was significantly longer than one would expect for a promoter.

The next step was to include a selection technique, as mentioned earlier in phase I, so PAC was included in the plasmid. Furthermore, to aid in the visualization of the transduction (and quantification), GFP was also included. However, GFP was replaced with its brighter counterpart, EGFP. With regards to Cas9 sequence, the default one was kept in the plasmid. Then the company (VectorBuilder) optimized the plasmid by providing a specific Cas9 sequence based on *Drosophila melanogaster* codons, so this is the one that was used in the final design of the plasmid. Although this sequence was not derived from *Apis mellifera* directly, the fruit fly genome is relatively highly conserved in comparison to the human genome, so it was preferred over the original Cas9 sequence.

Finally, with regards to the gRNA design, CRISPRflydesign was used to optimize the gRNA with regards to off-target and on-target sites. However, since honey bees were not available on it, nor on others such as CHOP-CHOP, Benchling was used instead. The beta-octopamine receptor 2 sequence was obtained from literature (Balfanz et al., 2014). This was then uploaded to Benchling. The honey bee genome was selected, and a list of all potential gRNAs was generated, each with its own off target and on target scores. Preference was shown for gRNAs that were towards the start of the sequence of the octopamine receptor. This was to avoid the potential of creating a truncated protein. The

gRNA sequence of choice is highlighted in the Figure below. The gRNA promoter of choice was dU6-3. This was the most expressed of the three U6 promoters that have been optimized for the fruit fly (Huynh, Depner, Larson, & King-Jones, 2020).

<input type="checkbox"/>	Position	Strand	Guide Sequence	PAM	On-Target Score	Off-Target Score
<input type="checkbox"/>	32	+	GACGAGCAGCGAATCGAGCG	AGG	63.8*	45.4
<input type="checkbox"/>	35	+	GAGCAGCGAATCGAGCGAGG	TGG	71.2*	43.4
<input type="checkbox"/>	44	+	ATCGAGCGAGGTGGTGTCTCT	CGG	49.8*	49.1
<input type="checkbox"/>	47	+	GAGCGAGGTGGTGTCTCTCGG	TGG	63.1*	49.6
<input type="checkbox"/>	50	-	CAGGGTCGTCACGTCCACCG	AGG	72.3*	50.0
<input type="checkbox"/>	68	-	GGTCGAGATGCCGTTCAACA	GGG	65.3*	48.7
<input type="checkbox"/>	69	+	GACGTGACGACCCTGTTGAA	CGG	49.1*	49.4
<input type="checkbox"/>	69	-	CGGTCGAGATGCCGTTCAAC	AGG	36.1*	48.8
<input type="checkbox"/>	83	+	GTTGAACGGCATCTCGACCG	AGG	72.6*	49.2
<input type="checkbox"/>	87	+	AACGGCATCTCGACCGAGGA	CGG	59.9*	48.5
<input type="checkbox"/>	89	-	CGTCCCAGCTGGCCGTCCT	CGG	48.0*	49.9
<input type="checkbox"/>	95	+	CTCGACCGAGGACGGCCAGC	TGG	40.7*	49.5
<input type="checkbox"/>	96	+	TCGACCGAGGACGGCCAGCT	GGG	49.3*	49.6
<input type="checkbox"/>	99	-	AGCTCGCGTTTCGTTCCCAGC	TGG	48.1*	49.4
<input type="checkbox"/>	122	+	GAACGGAGCTACTCGAGCG	AGG	67.2*	49.0
<input type="checkbox"/>	134	+	CTCGAGCGAGGAGAAGTTGT	CGG	55.9*	47.7
<input type="checkbox"/>	148	-	GACGTTTCAGGATCCCTCAG	AGG	56.0*	49.7

Figure 8. Benchling PAM and gRNA sequence output. The sequences are each assigned an offtarget score and on-target score. Higher is desirable for both scores. This figure shows a sub-section of the entire gRNA list of potential sequences, sorted by on-target and off-target scores, highest to lowest.

Each component needed a promoter. Each promoter must be maintained in order to have consistent expression, which further added complexity to the plasmid design. This was solved by using a T2A site, (*thosea asigna* virus 2A). In essence, this leads to the translation of multicistronic sequences, so multiple genes can be expressed using a single promoter. The mode of action can be observed in **Figure 9**, where the T2A causes the ribosomes to skip synthesis of the peptide bond that would normally connect the two proteins, Cas9 with the EGFP-PAC fusion protein, resulting in the synthesis of two separate proteins without the use of multiple promoters.

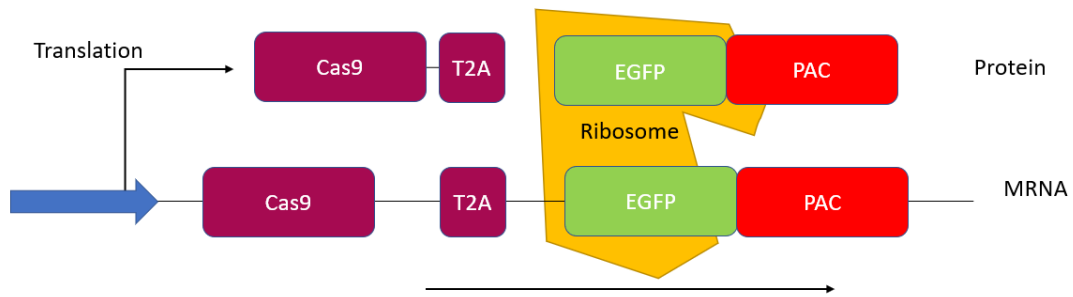


Figure 9. Schematic depicting how T2A leads to two separate proteins, using a single promoter. This graphic shows the mode of action of T2A as well as the location of the peptide bond that isn't synthesized.

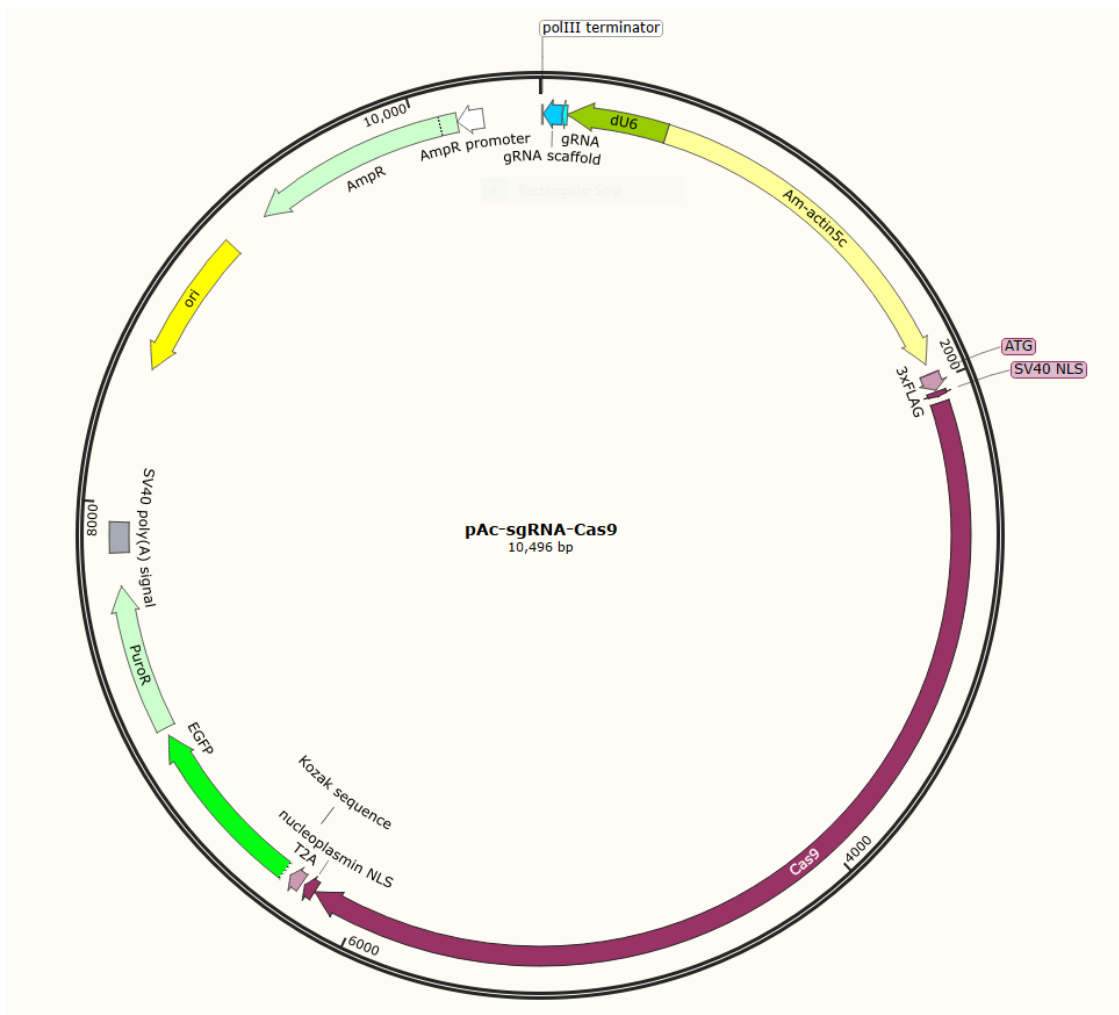


Figure 10. Schematic of the de novo finalized plasmid. The overall plasmid design containing all aforementioned components. The key components include: dU6, Am-actin5c, Cas9, EGFP-PuroR, Ori, sgRNA, PAM, and AmpR.

The final plasmid construct design can be observed in **Figure 11**. VectorBuilder suggested a few changes to the design, one important change was swapping out the AmCas9 with a DmCas9. Although it's the *Drosophila melanogaster* Cas9 counterpart, it should have more success when compared to the human codon optimized Cas9 as the fruit fly is more closely related to the honeybee. Another important item that was included, was the Tn7l and Tn7r elements. These elements allow for the integration of this plasmid into the baculovirus. PucOri replaced the Ori sequence that was originally included along with the addition of Gentamicin. These elements were essential for VectorBuilder to synthesize the plasmid and to ensure the successful knockdown of the octopamine beta sub-type 2 receptor.

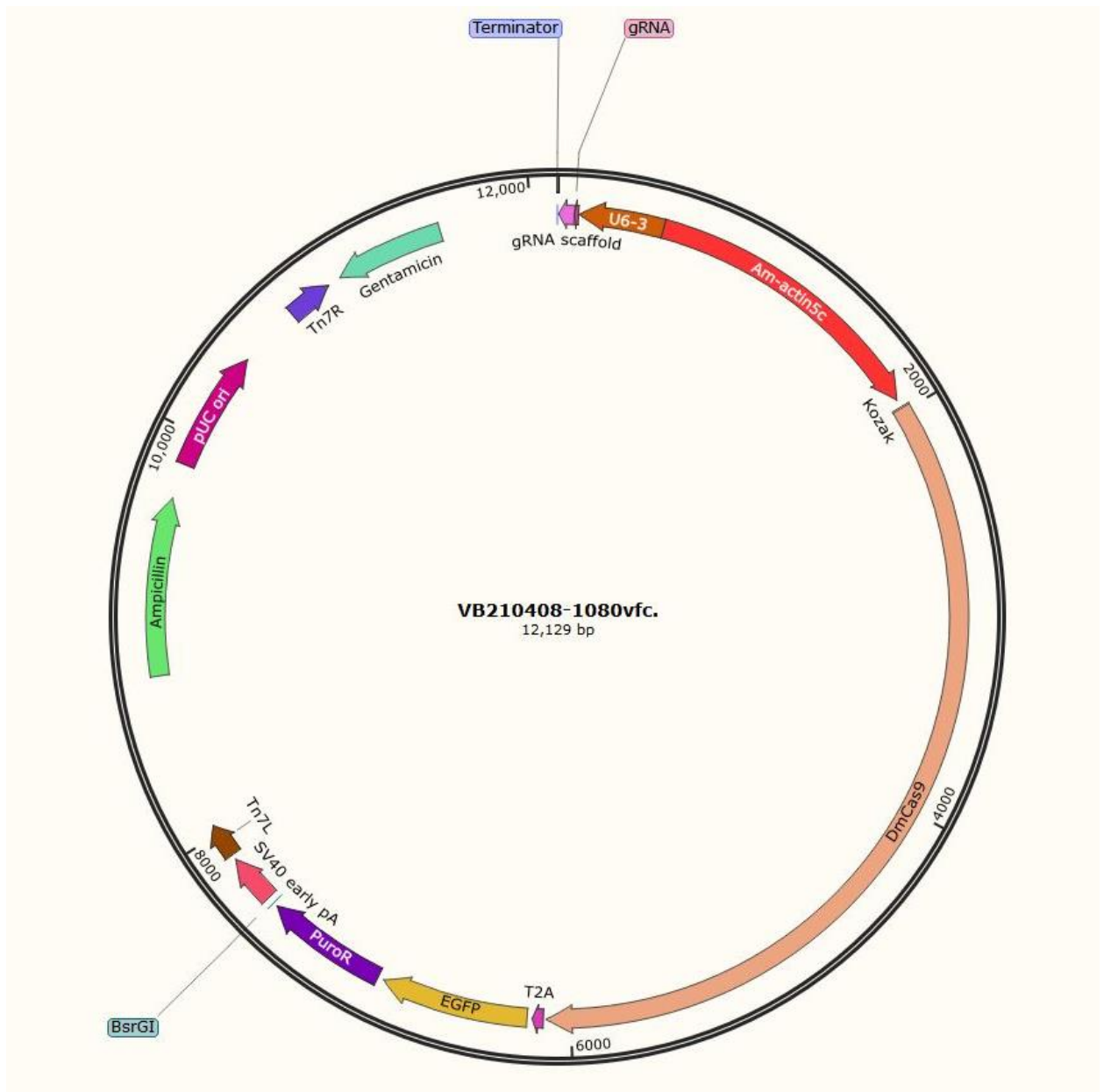


Figure 11. Plasmid with changes accommodating the request of the synthesizing company. A few minor additions were made to allow VectorBuilder to synthesize the plasmid, as well as increasing the likelihood of the knockdown. These changes included adding Gentamicin, as well as swapping the Cas9 with a DmCas9.

Transduction

Prior to transduction, the cells were split from a flask onto coverslips placed inside a 6 well plate. These cover slips will be treated with 1 - 2 ml of poly-l-lysine for 24 hours prior to adding the cells in order to facilitate the adhesion of cells. Upon achieving 80% confluency,

a calculation will be made depending on the PFU of baculovirus that we will receive. This calculation will then determine the amount of the baculovirus-packaged plasmid that will be added to the cells in each well. The cells will then be incubated at 32° C for 2 hr. After which imaging in a similar fashion to the methodology described above using the Ziess fluorescent microscope will be carried out, with and without fura-2.

4. Results

As expected trehalose levels were variable across all of the age classes. In newly emerged bees, fructose and trehalose injections caused an increase in glucose levels, while fucose, glucose, and sorbose caused a lowering of glucose levels. The fucose, fructose, and sorbose treatments lowered hemolymph trehalose levels. The remainder of the sugars in trehalose injected bees did not show any substantial differences. Sorbose injected bees exhibited lower sugar amounts when compared to the control. The glucose injected bees did not exhibit higher levels of glucose; however, they did have lower levels of fructose and glucose when compared to the control. The levels of fucose and trehalose are within the range of the standard error when compared to the control group. The fructose injected bees did not exhibit any change in the levels of fucose or fructose, when compared to the control group. However, trehalose appeared to decrease. The fucose injected bees did not show any meaningful change in the levels of fucose. However, fructose, trehalose and glucose were lower in the fucose injected bees (Figure 12).

In nurse bees injected with fucose, levels of the sugars did not exhibit any dramatic change as compared to the control group. Only glucose exhibited a slight increase outside the range of the standard error bars. An almost identical profile can be observed for the fructose injected nurse bees, however with slightly elevated levels of fructose. The glucose injected, again exhibited a similar level of sugars when compared to the control group. However, the trehalose measurements were slightly higher. The trehalose injected nurse bees showed a profile that, again, very closely resembles the control group. Finally, the sorbose injected

group, showed a similar trend to the one reported for the newly emerged bees where the sugar levels were decreased, with the exception of glucose (Figure 13).

Fucose injected foragers exhibited no change when compared to the control group. The fructose injected bees interestingly showed a profile where the fructose levels were higher than the control group. Although it's worthwhile noting that these changes were within the range of the standard error bars. The trehalose and glucose had a similar profile to that of the control. The fucose was slightly lower, although, again not outside the scope of the standard error bars. In the glucose injected group, the glucose and fructose levels were higher than that of the control group. This difference was such that the standard error bars did not overlap for either sugar. The trehalose and the fucose levels remained quite close to the levels in the control. The trehalose injected foragers exhibited the highest levels of trehalose, although this was paired with the largest standard error bar as well. The rest of the sugars, fucose, fructose, and glucose retained a similar profile to that of the control group. Finally, the sorbose injected forager bees, in a similar fashion to that of the newly emerged and nurse bees, exhibited lower levels of all four sugars (Figure 14).

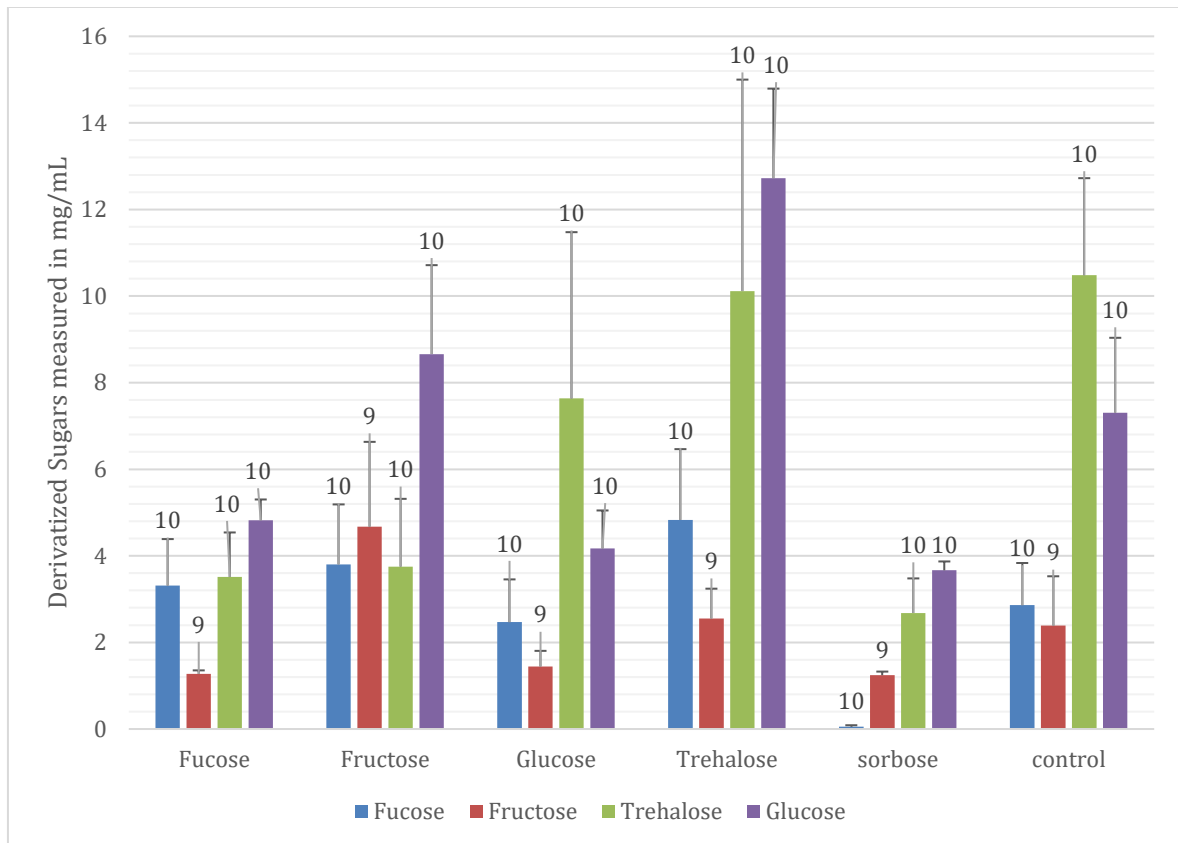


Figure 12. Newly emerged bees GC-MS sugar quantification. We measured 4 sugars, Fucose, Fructose, Trehalose, and Glucose. These sugars were measured after injecting the nurse bees with the six sugars: Fucose, Fructose, Glucose, Trehalose, Sorbose, and Ringer’s solution. Each bar represents the sugar content in the honey bee hemolymph, which error bars represent the standard error. The sample size is indicated above each respective bar.

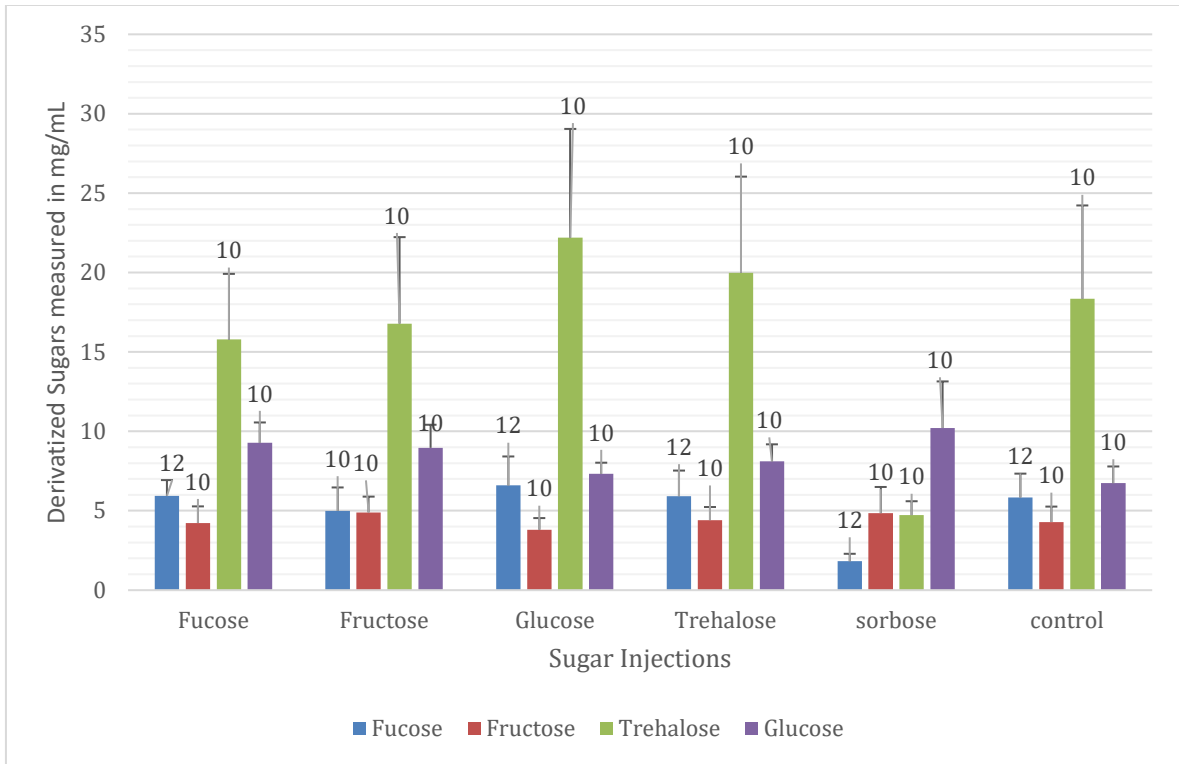


Figure 13. Nurse bees GC-MS sugar quantification. We measured 4 sugars, Fucose, Fructose, Trehalose, and Glucose. These sugars were measured after injecting the nurse bees with the six sugars: Fucose, Fructose, Glucose, Trehalose, Sorbose, and Ringer’s solution. Each bar represents the sugar content in the honey bee hemolymph, which error bars represent the standard error. The sample size is indicated above each respective bar.

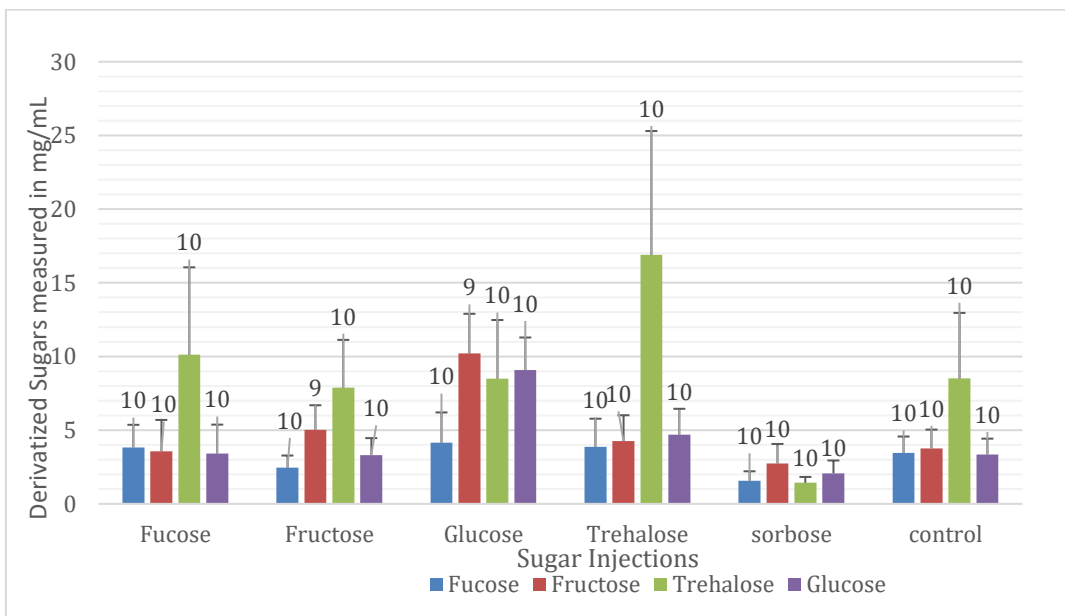


Figure 14. Forager bees GC-MS sugar quantification. We measured 4 sugars, Fucose, Fructose, Trehalose, and Glucose. These sugars were measured after injecting the nurse

bees with the six sugars: Fucose, Fructose, Glucose, Trehalose, Sorbose, and Ringer's solution. Each bar represents the sugar content in the honey bee hemolymph, which error bars represent the standard error. The sample size is indicated above each respective bar.

There was no significant difference of gene expression for ILP1 and ILP2 by sugar injections treatment (Kruskal Wallis test by treatment: $\chi^2_{3,103} = 1.18$, $P = 0.76$). or between each of the genes (Kruskal Wallis test by gene target: $\chi^2_{1,103} = 0.75$, $P = 0.39$) (Figure 15).

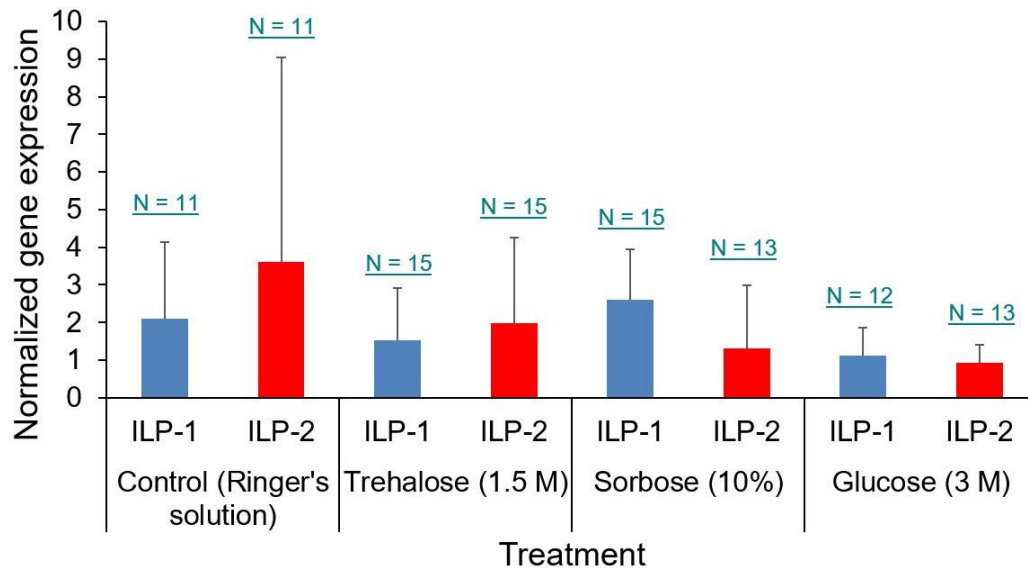


Figure 15. qPCR ILP-1 and ILP-2 gene expression results from forager bees. The foragers were injected with Ringer's solution (control), Trehalose (1.5M), Sorbose (10%), Glucose (3M) and then their gene expression of Insulin Like Protein (ILP)-1 and ILP-2 were measured. Mean and standard deviations of $\Delta\Delta CT$ values representing the normalized relative gene expression of ILP1 (blue) and ILP2 (red). The sample sizes are indicated above each bar.

There was computer colored images of cells with increased Fura-2 signaling after the agonist octopamine was added (Figure 16). Overall, there was a significant increase in calcium signaling in comparison to baseline levels after the agonist of 7 mM octopamine was added to the cell culture (Paired T-test: $df = 4$, $P = 0.034$, Figure 17).

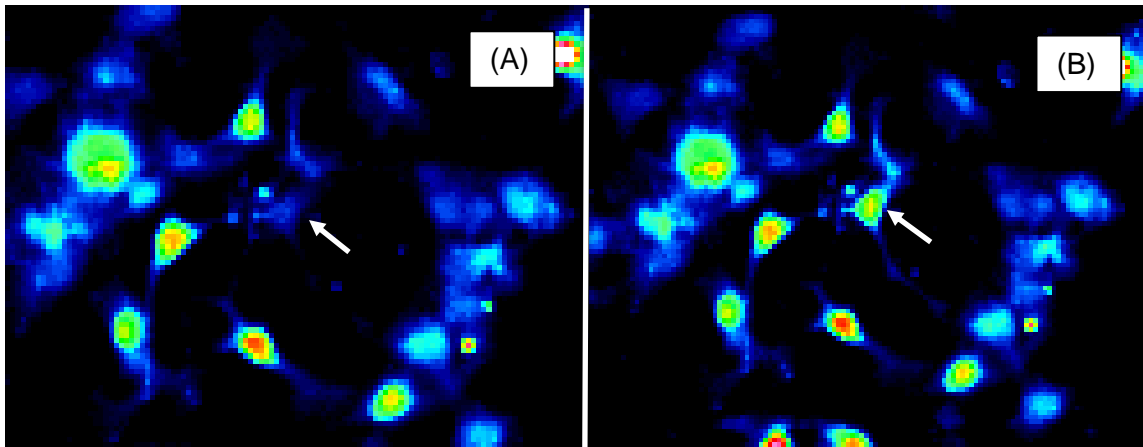


Figure 16. Live cell imaging of Fura-2 dyed Ame711 cells. Before (A) and after (B) Fura-2 stain of signal activation of one representative AME711 cell (arrow) using Octopamine at 7 mM concentration acting as the agonist. Signals were quantified at 20 x magnification.

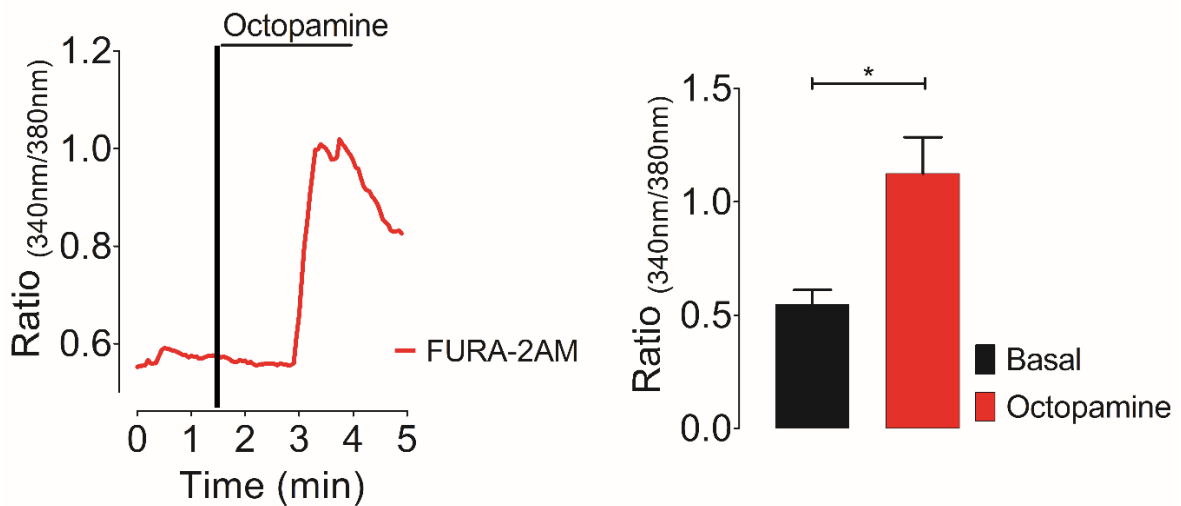


Figure 17. Ratio of the signals obtain from Fura-2AM (340/380nm) signaling. The graph on the right represents the average response of 5 cells to octopamine at 7 mM added at 1.5 minutes into the experiment. The bar graph on the right is a comparison between Basal levels and Maximum response of the cells to octopamine. * denotes significance at the alpha = 0.05 level.

5. Discussion

5.1 Sugar level manipulation confirmation

Previous studies have shown that GC-MS can be used to quantify the hemolymph sugar levels of the honey bee (Mayack et al., 2020). Here we used it to confirm if our sugar injections into the thorax of the honey bee were successful in manipulating the hemolymph sugar levels of the treated individuals. We confirmed that the injection with 10% sorbose leads to a lowering of trehalose levels in the hemolymph, and this is agreement with previous literature (Mayack & Naug, 2013; Roces & Blatt, 1999b). In fact, we observe this consistently in all age classes. This is probably due to the fact that it acts as a competitive inhibitor of trehalase p-synthase, which is responsible for synthesizing glucose into trehalose (Mayack et al., 2020). Surprisingly, fucose injected bees on the other hand did not result in higher fucose levels in the hemolymph for the newly emerged bees. This is a non-metabolizable sugar so it was predicted that the injected sugar would be stable in the hemolymph and not be metabolized (Roces & Blatt, 1999b). This is consistent with what has been reported previously, the crop load of fucose injected honey bees did not exhibit increased amounts of fucose, though it was expected to increase (Roces & Blatt, 1999a). However, we are detecting fucose in all of the treated bees except the sorbose injected bees, which leads us to believe that the peak chosen for this sugar may not be accurate. Based on previous literature, we do not expect to see fucose in the hemolymph. Fructose levels are the highest in the fructose injected bees, which is to be expected. However, it is interesting to note how trehalose injections in newly emerged bees resulted in an increase in the levels of glucose, yet the glucose injected bees have lower levels in comparison to the control bees, but higher trehalose levels. This could be due to an increase in the breakdown of trehalose if the bees were stressed due to the harnessing, as stressed bees need to immobilize more of their fat reserves in order to maintain their energetic demands, this is in the form of converting the fat reserves into molecules that are ready for consumption, this molecule being trehalose (Woodring et al., 1993). In turn, glucose is used by the cells ultimately, but the

conversion from trehalose to glucose can outpace this demand (Abou-Seif et al., 1993). Glucose in the hemolymph should be regulated, potentially providing an explanation for the lack of increase in these treated bees as it is normally converted to trehalose if there is any excess amount of it (Jasmina Blatt & Roces, 2001a) and the glucose treated bees have higher trehalose levels in comparison to the control bees. The lack of sugar level manipulation in the expected directions is one possible explanation for only observing significant appetite differences in the fucose and sorbose treated newly emerged bees. However, more samples need to be analyzed by GC-MS to increase the statistical power of the comparisons shown here.

In the nurse bees, the most striking observation in relation to the manipulation of sugar levels from injections is the consistently high trehalose levels across all treatments except for the sorbose treated bees. We suspected this was due to the nurse bees being under stress, which may have resulted in the release of octopamine, hypertrehalosic hormone, or adipokinetic hormone that can mobilize the fat stores of the nurse bees (Wang et al., 2012). The mobilization from these hormones usually results in an increase in trehalose levels (Park & Keeley, 1998). In general, nurse bees have better capacity to buffer against energetic stress, and their appetite levels tend to be lower in comparison to the newly emerged and forager age classes, so our findings were not surprising as this age class appears to be able to better regulate their energetic state on an individual level (Wang et al., 2012). However, stressed bees usually have elevated levels of trehalose as it acts as a ready energy supply for fight or flight situations because it can be quickly mobilized into glucose (Wang et al., 2012). The lack of sugar level differences in the nurse bees might aid in explaining why we did not see any appetite differences across all of the treatments for this age class. Despite the lowering of the trehalose in this age class it did not result in the increase of appetite as originally predicted.

In the forager age class, we have the clearest evidence that we have control over manipulating the sugar levels via injections. The levels were manipulated in the expected manner except for fructose. The levels of trehalose in injected bees, when compared to the levels of trehalose in control, are twofold higher. Furthermore, relative to other

sugars in the same injection, trehalose levels were almost always the highest. Trehalose is the primary “blood sugar” of the honey bee (S. Nelson Thompson, 2003), which enables us to observe their energetic demands, this was concluded after observing the levels of trehalose, glucose and fructose under high metabolic load, finding that the levels of glucose and fructose remained constant, while the levels of trehalose fluctuated with changing metabolic rates (J. Blatt & Roces, 2002). It is a well-known fact that honey bee energetic demands vary across their differing age groups, with foragers requiring significantly more energy, with lower fat stores (J. M. Harrison, 1986). The foragers need to maintain a raised temperature surrounding their thorax, in order to enable the forager bees to take flight at short notice, and this further contributes to their increased energetic demands (Stabentheiner & Kovac, 2014). Finally, compared to other age groups, the foragers carry out more demanding tasks, such as leaving the hive and travelling 3.2 km on average in order to forage for pollen and nectar.

This is also the case of glucose in glucose injected bees when compared to the control, where the increase is also about twofold higher. Compared to previous literature, we see that sugar levels relative to each other are in line with what has been reported (Jasmina Blatt & Roces, 2001b). The authors observed that in the foragers, trehalose levels tended to be much higher in mg/ml when compared the levels of other sugars. Furthermore, upon direct comparison of trehalose levels, there were similar levels recorded for trehalose, glucose, and fructose. We are, therefore, most confident in the sugar manipulation carried out for the foraging age class, and this also corresponds to much more dramatic differences in appetite based on the sugar injection treatment with fucose and sorbose causing significant increases in appetite. In summary, more extensive measures need to be taken to ensure the accurate manipulation of sugar levels in the newly emerged and nurse bee age class in order to study their effects on appetite regulation. Moreover, more samples will be run to increase the sample sizes and statistical power to confirm if the differences observed are significant from one another.

There were no significant differences in the expression of ILP-1 and ILP-2 for forager bees injected with 10% sorbose, trehalose (1.5 M) and glucose (3 M). These results

suggest that the appetite differences observed resulting from a lowering of trehalose from the 10% sorbose treatment, via the increase of octopamine and the lowering of tyramine levels in the brain, are independent of the glucose-insulin pathway.

Similar to previous expression studies carried out on insulin-like proteins, in ringer's treated foragers the ILP-2 expression was higher than ILP-1 (de Azevedo & Hartfelder, 2008; Wang et al., 2012). In fact, it has been suggested that the insulin-like proteins are responsible for caste development in the honey (de Azevedo & Hartfelder, 2008; Wang et al., 2012). In previous studies there was also high variation in the expression of these two genes which corresponds to what we observe, suggesting that an increase in sample size is not likely to yield significant differences (Nilsen et al., 2011). These facts combined are quite exciting as it suggests the insulin-like proteins are not the regulators of appetite. Although the bees were injected with trehalose and glucose, both metabolizable sugars, they did not exhibit any changes in the levels of expression of the insulin-like proteins. This retains the possibility that octopamine may be, in fact, the regulator of appetite, which is an alternative regulatory mechanism for appetite that we do not see in vertebrates.

The forager bees were injected with trehalose 1.5 M and 10% sorbose, after which octopamine in the brain was quantified. We can see that in the foragers 10% sorbose injections were associated with significantly higher levels of octopamine and lower levels of tyramine (Figure S5). Meaning that it is very likely that octopamine or tyramine are responsible for increase in the forager bee's appetite. It is interesting to note that higher trehalose levels in the forager bees did not result in the lowering of octopamine levels in the brain. Therefore, there appears to be only a signaling pathway for the lowering of trehalose levels to increase the appetite of the bee, but not a mechanism to induce the opposite effect when the trehalose levels are high.

There is high variation within the sugar level treatments. We suspect that a lot of variation can be attributed to the sample derivatization steps. This is actually confirmed in literature, where it was also pointed out that the derivatization of the samples resulted in more variation (Feil & Lunn, 2018). Therefore, I plan to analyze more samples in the

future to increase the statistical power in order to detect significant differences across the sugar levels from the treated bees.

5.2 Fura-2 imaging

Fura-2 requires a loading of the agonist into the cells, which was achieved successfully (Figure S3). However, the initial agonist used to load the cells was ATP, and there was no signal was detected. Octopamine receptor signaling in the honey bee cell line is calcium dependent. CAMKII is directly connected to the octopamine beta receptor; therefore, we expect that if we induce the octopamine receptor activity with octopamine, Fura-2 imaging can be used to visualize the signaling pathway suggested by the *Drosophila melanogaster* gene-gene interaction network. CAMKII is a Ca^{2+} /calmodulin dependent protein kinase II (Lisman, 1994). We knew that if the octopamine receptor was activated then downstream of this, we expected to detect the calcium signaling.

Furthermore, previous literature has been found to support this notion in *Drosophila melanogaster*, wherein activating the octopamine receptor results in an increase of Ca^{2+} ions (Blenau et al., 2020). Hence, I hypothesized that this is very likely to be the case for *Apis mellifera* as well, wherein Fura-2 imaging will allow the visualization of CAMKII activity and hence, at least indirectly, if not directly, allow the observation of the octopamine receptor signal transduction. Previous literature had employed a similar approach where fruit fly orthologs were applied to the honey bee (Schulte et al., 2013). Furthermore, another function that this imaging experiment served is that it allowed for the confirmation of the presence of the octopamine receptor in the AME711 cell line. Compared to previous Fura-2 experiments carried out on *Drosophila melanogaster*, similar signal behavior can be observed; however, the signal ratios reported in *Drosophila melanogaster* were higher than the ratios obtained, which can be attributed to many factors, from using an entirely different species of cells, to varying concentrations of agonists. More importantly, the studies use cells that are expressing the recombinant protein at very high levels, further explaining the difference observed in the signal intensities (Hu et al., 1994). There was evidence of activating calcium signaling using octopamine as the agonist. Many of the cells exhibited the signal and shortly after the introduction of octopamine as there was a spike in the signal. The response, when

compared to basal levels, is significantly higher after adding the agonist. In addition, more endogenously and exogenously activated calcium signals from cells were documented. This indicates that the Ame711 cell line is naturally in fact quite active, at least in terms of calcium signaling. The remainder of the spikes in signal were after the 1.5-minute marker indicating that they were in fact induced using exogenous octopamine. This confirms that the Ame711 cell line may be used for the purpose of studying signaling in honey bees, at least for studying calcium signaling. Finally, this experiment confirms the presence of octopamine receptors indirectly, an important step before carrying out a knockdown of the octopamine beta subtype 2 receptor. Finally, this was a relevant experiment to carry out in order to be able to demonstrate that this, newly established cell line, does in fact have active signaling mechanisms, which further indicates that this cell line can aid future *in vitro* studies to be carried out on *Apis mellifera*.

Future studies

In the future using LC-MS instead of GC-MS might help with reducing the variability across samples within a treatment group. With GC-MS the hemolymph sugars could not be directly quantified, and hence they require derivatization that involves adding one or more trimethylsilyl groups to the sugar. Although these differences in derivatized sugar concentrations may seem insignificant, the differences are amplified because the GC-MS is a very sensitive instrument for the detection of sugars.

With the plasmid developed in this study, a potential anti-viral treatment for deformed wing virus could be developed. This virus is one of the most damaging factors contributing to the most recent bee health declines around the world (Posada-Florez et al., 2019). The plasmid sequence I have designed along with the baculovirus vector could be modified to genetically engineer the honey bee to synthesize antiviral proteins endogenously. Compared to previous studies, this would be quite advantageous over siRNA treatments because they have possible off-target effects, whereas antiviral protein function and the intended target is much better understood. Previous literature has already shown that some insects already produce antiviral proteins (Chernysh et al., 2002). In addition, with regards

to Fura-2 testing, this was an important first step that confirms the presence calcium-based signal transduction occurring in the AME711 cell line, allowing for future studies on the aforementioned pathways to be carried out. Another step towards increasing the widespread use of the cell line would be to immortalize the cell line using pre-existing commercially available plasmids in order to induce a proto-oncogene in the established AME711 cell line (Brooks, James, Patek, Williamson, & Arends, 2001).

BIBLIOGRAPHY

- Abou-Seif, M. A. M., Maier, V., Fuchs, J., Mezger, M., Pfeiffer, E. F., & Bounias, M. (1993). Fluctuations of carbohydrates in haemolymph of honey bee (*Apis mellifera*) after fasting, feeding and stress. *Hormone and Metabolic Research*, 25, 4-8.
- Axelrod, J., & Saavedra, J. M. (1977). Octopamine. *Nature*, 265(5594), 501-504.
doi:10.1038/265501a0
- Balfanz, S., Jordan, N., Langenstück, T., Breuer, J., Bergmeier, V., & Baumann, A. (2014). Molecular, pharmacological, and signaling properties of octopamine receptors from honey bee (*Apis mellifera*) brain. *Journal of Neurochemistry*, 129(2), 284-296.
doi:<https://doi.org/10.1111/jnc.12619>
- Bassett, A. R., Tibbit, C., Ponting, C. P., & Liu, J. L. (2014). Mutagenesis and homologous recombination in *Drosophila* cell lines using CRISPR/Cas9. *Biol Open*, 3(1), 42-49.
doi:10.1242/bio.20137120
- Bitterman, M. E., Menzel, R., Fietz, A., & Schäfer, S. (1983). Classical conditioning of proboscis extension in honey bees (*Apis mellifera*). *Journal of Comparative Psychology*, 97(2), 107-119. doi:10.1037/0735-7036.97.2.107
- Blatt, J., & Roces, F. (2001a). Haemolymph sugar levels in foraging honey bees (*Apis mellifera carnica*): dependence on metabolic rate and in vivo measurement of maximal rates of trehalose synthesis. *Journal of Experimental Biology*, 204, 2709-2716.
- Blatt, J., & Roces, F. (2001b). Haemolymph sugar levels in foraging honey bees (*Apis mellifera carnica*): dependence on metabolic rate and in vivo measurement of maximal rates of trehalose synthesis. *Journal of Experimental Biology*, 204(15), 2709-2716. doi:10.1242/jeb.204.15.2709
- Blatt, J., & Roces, F. (2002). The control of the proventriculus in the honey bee (*Apis mellifera carnica* L.) I. A dynamic process influenced by food quality and quantity? *J Insect Physiol*, 48(6), 643-654. doi:10.1016/s0022-1910(02)00090-2
- Blenau, W., Wilms, J. A., Balfanz, S., & Baumann, A. (2020). AmOct α 2R: Functional Characterization of a Honey bee Octopamine Receptor Inhibiting Adenylyl Cyclase

- Activity. *International Journal of Molecular Sciences*, 21(24), 9334. Retrieved from <https://www.mdpi.com/1422-0067/21/24/9334>
- Brooks, D. G., James, R. M., Patek, C. E., Williamson, J., & Arends, M. J. (2001). Mutant K-ras enhances apoptosis in embryonic stem cells in combination with DNA damage and is associated with increased levels of p19ARF. *Oncogene*, 20(17), 2144-2152. doi:10.1038/sj.onc.1204309
- Chan, M. M., Choi, S. Y., Chan, Q. W., Li, P., Guarna, M. M., & Foster, L. J. (2010). Proteome profile and lentiviral transduction of cultured honey bee (*Apis mellifera* L.) cells. *Insect Mol Biol*, 19(5), 653-658. doi:10.1111/j.1365-2583.2010.01022.x
- Chan, Q. W., Howes, C. G., & Foster, L. J. (2006). Quantitative comparison of caste differences in honey bee hemolymph. *Mol Cell Proteomics*, 5(12), 2252-2262. doi:10.1074/mcp.M600197-MCP200
- Chernysh, S., Kim, S. I., Bekker, G., Pleskach, V. A., Filatova, N. A., Anikin, V. B., . . . Bulet, P. (2002). Antiviral and antitumor peptides from insects. *Proceedings of the National Academy of Sciences*, 99(20), 12628-12632. doi:10.1073/pnas.192301899
- de Azevedo, S. V., & Hartfelder, K. (2008). The insulin signaling pathway in honey bee (*Apis mellifera*) caste development — differential expression of insulin-like peptides and insulin receptors in queen and worker larvae. *Journal of Insect Physiology*, 54(6), 1064-1071. doi:<https://doi.org/10.1016/j.jinsphys.2008.04.009>
- Eagle, H. (1955). Nutrition needs of mammalian cells in tissue culture. *Science*, 122(3168), 501-514. doi:10.1126/science.122.3168.501
- Farooqui, T., Vaessin, H., Smith, B.H., 2004. Octopamine receptors in the honeybee (*Apis mellifera*) brain and their disruption by RNA-mediated interference. *J Insect Physiol* 50, 701-713.
- Feil, R., & Lunn, J. E. (2018). Quantification of Soluble Sugars and Sugar Alcohols by LC-MS/MS. In C. António (Ed.), *Plant Metabolomics: Methods and Protocols* (pp. 87-100). New York, NY: Springer New York.
- Gazi, L., Nickolls, S. A., & Strange, P. G. (2003). Functional coupling of the human dopamine D2 receptor with Gai1, Gai2, Gai3 and Gao G proteins: evidence for agonist regulation of G protein selectivity. *British Journal of Pharmacology*, 138(5), 775-786. doi:<https://doi.org/10.1038/sj.bjp.0705116>

- Goblirsch, M. J., Spivak, M. S., & Kurtti, T. J. (2013). A Cell Line Resource Derived from Honey Bee (*Apis mellifera*) Embryonic Tissues. *PLOS ONE*, 8(7), e69831. doi:10.1371/journal.pone.0069831
- Grohmann, L., Blenau, W., Erber, J., Ebert, P. R., Strünker, T., & Baumann, A. (2003). Molecular and functional characterization of an octopamine receptor from honey bee (*Apis mellifera*) brain. *Journal of Neurochemistry*, 86(3), 725-735. doi:<https://doi.org/10.1046/j.1471-4159.2003.01876.x>
- Grynkiewicz, G., Poenie, M., & Tsien, R. Y. (1985). A new generation of Ca²⁺ indicators with greatly improved fluorescence properties. *J Biol Chem*, 260(6), 3440-3450.
- Harrison, J. M. (1986). Caste-Specific Changes in Honey bee Flight Capacity. *Physiological Zoology*, 59(2), 175-187. doi:10.1086/physzool.59.2.30156031
- Harrison, R. G. (1906). Observations on the living developing nerve fiber. *Proceedings of the Society for Experimental Biology and Medicine*, 4(1), 140-143. doi:10.3181/00379727-4-98
- Horodecka, K., & Döchler, M. (2021). CRISPR/Cas9: Principle, Applications, and Delivery through Extracellular Vesicles. *International Journal of Molecular Sciences*, 22(11), 6072. Retrieved from <https://www.mdpi.com/1422-0067/22/11/6072>
- Hu, Y. F., Vaca, L., Zhu, X., Birnbaumer, L., Kunze, D. L., & Schilling, W. P. (1994). Appearance of a Novel Ca²⁺ Influx Pathway in Sf9 Insect Cells Following Expression of the Transient Receptor Potential-like (trpl) Protein of *Drosophila*. *Biochemical and Biophysical Research Communications*, 201(2), 1050-1056. doi:<https://doi.org/10.1006/bbrc.1994.1808>
- Huynh, N., Depner, N., Larson, R., & King-Jones, K. (2020). A versatile toolkit for CRISPR-Cas13-based RNA manipulation in *Drosophila*. *Genome Biology*, 21(1), 279. doi:10.1186/s13059-020-02193-y
- Ikeda, T., Nakamura, J., Furukawa, S., Chantawannakul, P., Sasaki, M., & Sasaki, T. (2011). Transduction of baculovirus vectors to queen honey bees, *Apis mellifera*. *Apidologie*, 42(4), 461. doi:10.1007/s13592-011-0014-z
- Kalesnykas, G., Kokki, E., Alasaarela, L., Lesch, H., Tuulos, T., Kinnunen, K., . . . Ylä-Herttuala, S. (2017). Comparative Study Of Adeno-Associated Virus, Adenovirus,

- Baculovirus And Lentivirus Vectors For Gene Therapy Of The Eyes. *Current gene therapy*, 17. doi:10.2174/1566523217666171003170348
- Korst, P. J. A. M., & Velthuis, H. H. W. (1982). The nature of trophallaxis in honey bees. *Insectes Sociaux*, 29(2), 209-221. doi:10.1007/BF02228753
- Kost, T. A., Condreay, J. P., & Jarvis, D. L. (2005). Baculovirus as versatile vectors for protein expression in insect and mammalian cells. *Nature Biotechnology*, 23(5), 567-575. doi:10.1038/nbt1095
- Lisman, J. (1994). The CaM kinase II hypothesis for the storage of synaptic memory. *Trends in Neurosciences*, 17(10), 406-412. doi:[https://doi.org/10.1016/0166-2236\(94\)90014-0](https://doi.org/10.1016/0166-2236(94)90014-0)
- Luyckx, J., & Baudouin, C. (2011). Trehalose: an intriguing disaccharide with potential for medical application in ophthalmology. *Clin Ophthalmol*, 5, 577-581. doi:10.2147/opth.S18827
- Massotte, D. (2003). G protein-coupled receptor overexpression with the baculovirus–insect cell system: a tool for structural and functional studies. *Biochimica et Biophysica Acta (BBA) - Biomembranes*, 1610(1), 77-89. doi:[https://doi.org/10.1016/S0005-2736\(02\)00720-4](https://doi.org/10.1016/S0005-2736(02)00720-4)
- Mayack, C., Carmichael, K., Phalen, N., Khan, Z., Hirche, F., Stangl, G. I., & White, H. K. (2020). Gas chromatography – Mass spectrometry as a preferred method for quantification of insect hemolymph sugars. *Journal of Insect Physiology*, 127, 104115. doi:<https://doi.org/10.1016/j.jinsphys.2020.104115>
- Mayack, C., & Naug, D. (2013). Individual energetic state can prevail over social regulation of foraging in honey bees. *Behavioral Ecology and Sociobiology*, 67(6), 929-936. doi:10.1007/s00265-013-1517-6
- Mayack, C., Phalen, N., Carmichael, K., White, H. K., Hirche, F., Wang, Y., . . . Amdam, G. V. (2019). Appetite is correlated with octopamine and hemolymph sugar levels in forager honey bees. *Journal of Comparative Physiology A*, 205(4), 609-617. doi:10.1007/s00359-019-01352-2
- Millar, N. S., Baylis, H. A., Reaper, C., Bunting, R., Mason, W. T., & Sattelle, D. B. (1995). Functional expression of a cloned *Drosophila* muscarinic acetylcholine

- receptor in a stable *Drosophila* cell line. *Journal of Experimental Biology*, 198(9), 1843-1850. doi:10.1242/jeb.198.9.1843
- Miller, T. A. (1997). Control of circulation in insects. *General Pharmacology: The Vascular System*, 29(1), 23-38. doi:[https://doi.org/10.1016/S0306-3623\(96\)00522-8](https://doi.org/10.1016/S0306-3623(96)00522-8)
- Nilsen, K.-A., Ihle, K. E., Frederick, K., Fondrk, M. K., Smedal, B., Hartfelder, K., & Amdam, G. V. (2011). Insulin-like peptide genes in honey bee fat body respond differently to manipulation of social behavioral physiology. *The Journal of experimental biology*, 214(Pt 9), 1488-1497. doi:10.1242/jeb.050393
- Park, J. H., & Keeley, L. L. (1998). The effect of biogenic amines and their analogs on carbohydrate metabolism in the fat body of the cockroach *Blaberus discoidalis*. *General and Comparative Endocrinology*, 110(1), 88-95. doi:10.1006/gcen.1997.7053
- Posada-Florez, F., Childers, A. K., Heerman, M. C., Egekwu, N. I., Cook, S. C., Chen, Y., . . . Ryabov, E. V. (2019). Deformed wing virus type A, a major honey bee pathogen, is vectored by the mite *Varroa destructor* in a non-propagative manner. *Scientific Reports*, 9(1), 12445. doi:10.1038/s41598-019-47447-3
- Roces, F., & Blatt, J. (1999a). Haemolymph sugars and the control of the proventriculus in the honey bee *Apis mellifera*. *Journal of Insect Physiology*, 45, 221-229.
- Roces, F., & Blatt, J. (1999b). Haemolymph sugars and the control of the proventriculus in the honey bee *Apis mellifera* Dedicated to Prof. Josué A. Núñez on the occasion of his 74th anniversary.1. *Journal of Insect Physiology*, 45(3), 221-229. doi:[https://doi.org/10.1016/S0022-1910\(98\)00116-4](https://doi.org/10.1016/S0022-1910(98)00116-4)
- Scheiner, R., Plückhahn, S., Oney, B., Blenau, W., & Erber, J. (2002). Behavioural pharmacology of octopamine, tyramine and dopamine in honey bees. *Behav Brain Res*, 136(2), 545-553. doi:10.1016/s0166-4328(02)00205-x
- Schulte, C., Lebouille, G., Otte, M., Grünewald, B., Gehne, N., & Beye, M. (2013). Honey bee promoter sequences for targeted gene expression. *Insect Mol Biol*, 22(4), 399-410. doi:10.1111/imb.12031
- Shah, K. S., Evans, E. C., & Pizzorno, M. C. (2009). Localization of deformed wing virus (DWV) in the brains of the honey bee, *Apis mellifera* Linnaeus. *Virology Journal*, 6(1), 182. doi:10.1186/1743-422X-6-182

- Simpson, S. J., & Raubenheimer, D. (1993). The central role of the haemolymph in the regulation of nutrient intake in insects. *Physiological Entomology*, 18(4), 395-403. doi:<https://doi.org/10.1111/j.1365-3032.1993.tb00613.x>
- Stabentheiner, A., & Kovac, H. (2014). Energetic Optimisation of Foraging Honey bees: Flexible Change of Strategies in Response to Environmental Challenges. *PLOS ONE*, 9(8), e105432. doi:10.1371/journal.pone.0105432
- Stacey, G., & Possee, R. (1996). Safety aspects of insect cell culture. *Cytotechnology*, 20(1-3), 299-304. doi:10.1007/bf00350409
- Thompson, S. N. (2003). Trehalose - The insect 'blood' sugar. *Advances in Insect Physiology*, 31, 205-285. Retrieved from <http://www.sciencedirect.com/science/article/pii/S0065280603310045>
- Thompson, S. N. (2003). Trehalose – The Insect ‘Blood’ Sugar. In *Advances in Insect Physiology* (Vol. 31, pp. 205-285): Academic Press.
- Thurtle-Schmidt, D. M., & Lo, T. W. (2018). Molecular biology at the cutting edge: A review on CRISPR/CAS9 gene editing for undergraduates. *Biochem Mol Biol Educ*, 46(2), 195-205. doi:10.1002/bmb.21108
- van der Sluijs, J. P., & Vaage, N. S. (2016). Pollinators and Global Food Security: the Need for Holistic Global Stewardship. *Food Ethics*, 1(1), 75-91. doi:10.1007/s41055-016-0003-z
- Wang, Y., Brent, C. S., Fennern, E., & Amdam, G. V. (2012). Gustatory Perception and Fat Body Energy Metabolism Are Jointly Affected by Vitellogenin and Juvenile Hormone in Honey Bees. *PLOS Genetics*, 8(6), e1002779. doi:10.1371/journal.pgen.1002779
- Woodring, J., Boulden, M., Das, S., & Gäde, G. (1993). Studies on blood sugar homeostasis in the honey bee (*Apis mellifera*, L.). *Journal of Insect Physiology*, 39(1), 89-97. Retrieved from <http://www.sciencedirect.com/science/article/B6T3F-49N9S7C-2SW/2/d45d8a724c8db15652334afc515d3467>
- Youn, H., Kirkhart, C., Chia, J., & Scott, K. (2018). A subset of octopaminergic neurons that promotes feeding initiation in *Drosophila melanogaster*. *PLOS ONE*, 13(6), e0198362. doi:10.1371/journal.pone.0198362

Zhao, Z. J., Chi, Q. S., Cao, J., & Han, Y. D. (2010). The energy budget, thermogenic capacity and behavior in Swiss mice exposed to a consecutive decrease in temperatures. *Journal of Experimental Biology*, 213(23), 3988-3997.
doi:10.1242/jeb.046821

Appendix A – Chemicals

Chemicals and contents	Supplier
Blastaq Green 2x qPCR	abm, Canada
BSTFA 1% TMCS	Thermo Scientific, USA
Fetal Bovine Serum	Sigma, Germany
Fucose	Sigma, Germany
Fura-2	Invitrogen, USA
Glucose	Sigma, Germany
Hexachlorobenzene	Sigma, Germany
Lavender oil	Arifoglu, Turkey
Low MW DNA ladder	New England Biolabs, USA
Millipore water	Merck Millipore, USA
Octopamine-Hydrochloric acid	Sigma, Germany
Pen/Strep Amphotericin B	Lonza, USA
Poly-l-lysine 0.01%	Sigma, Germany
Pyridine	Sigma, Germany
Schneider's Insect medium	Sigma, Germany
Sorbose	Sigma, Germany
Sucrose	Sigma, Germany
Trehalose	Sigma, Germany
Trypsin/EDTA	WISENT, Canada

Appendix B – Equipment

6-well plate	CellStar, Greiner Bio-One, Germany
Balance	PA224C, Ohaus, USA
Centrifuge	5425, Eppendorf, Germany
Dry ice maker	SnowPack, Burkle, Germany
Flasks 25ml	CellStar, Greiner Bio-One, Germany
Freeze Dryer	Teknosem, Turkey
Hot plate	MSH-20D, Witeg, Germany
Ice Machine	AF20, Scotsman Inc, USA
Incubator	Binder, Germany
Laminar Flow	HeraSafe HS 15, Heraeus, Germany
Light microscope	Primovert, Zeiss, Germany
Microliter pipettes	Eppendorf, Germany
Microliter pipettes	Capp, Denmark
Microwave	Arcelik, Turkey
Mini Centrifuge	myFuge, Benchmark sci. USA
Stereomicroscope	Stemi 305, Zeiss, Germany
Spectrophotometer	Nanodrop 2000, Thermofisher, USA
Vortex	VTX-3000L, LMS, Japan
Water Bath	NB 20, Nuve, Turkey

Appendix C – Biological Kits

OneScript cDNA synthesis Kit

abm, Canada

RNA extraction Kit

abm, Canada

Appendix D - Supplemental Figures

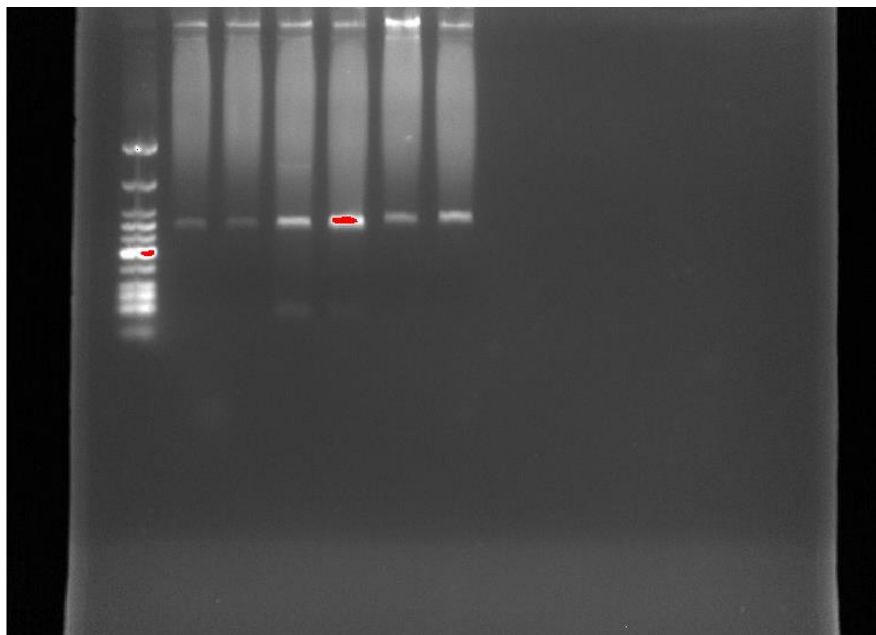


Figure S1. ILP1 Primer validation gel electrophoresis. Lane 1- Low Molecular Weight Ladder, Lane 2- S10 sample with ILP1 primers as positive control, Lane 3- S12 Sample with ILP1 primers as positive control, Lane 4- S10 sample with ILP2-1 primers, Lane 5- S12 sample with ILP2-1 primers, Lane 6- S10 sample with ILP2-3 primers, Lane 7- S12 sample with ILP2-3 primers.

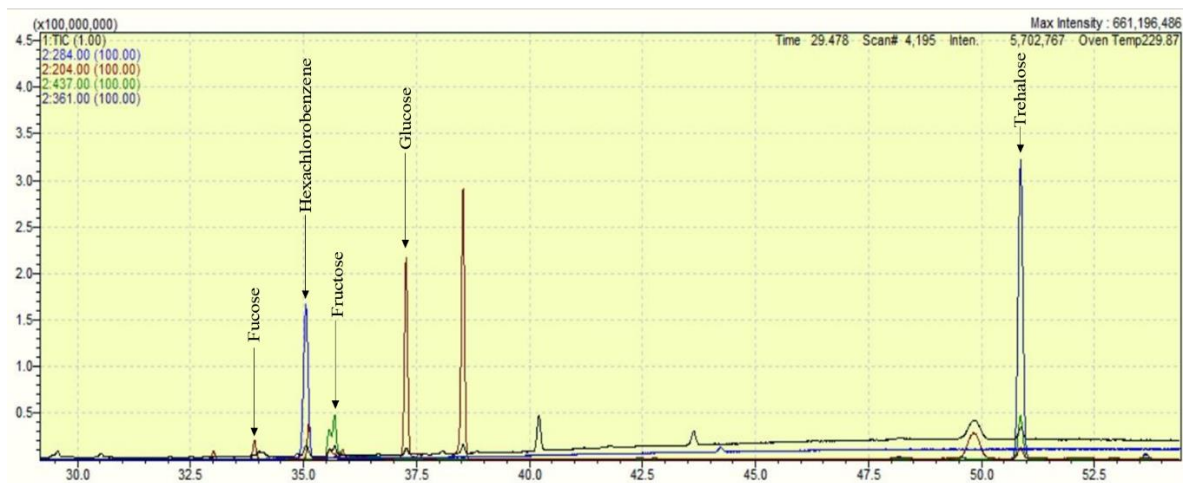


Figure S2. A representative chromatogram from the GC-MS sugar analysis. The peak of each sugar that was quantified is labelled along with the internal standard hexachlorobenzene.

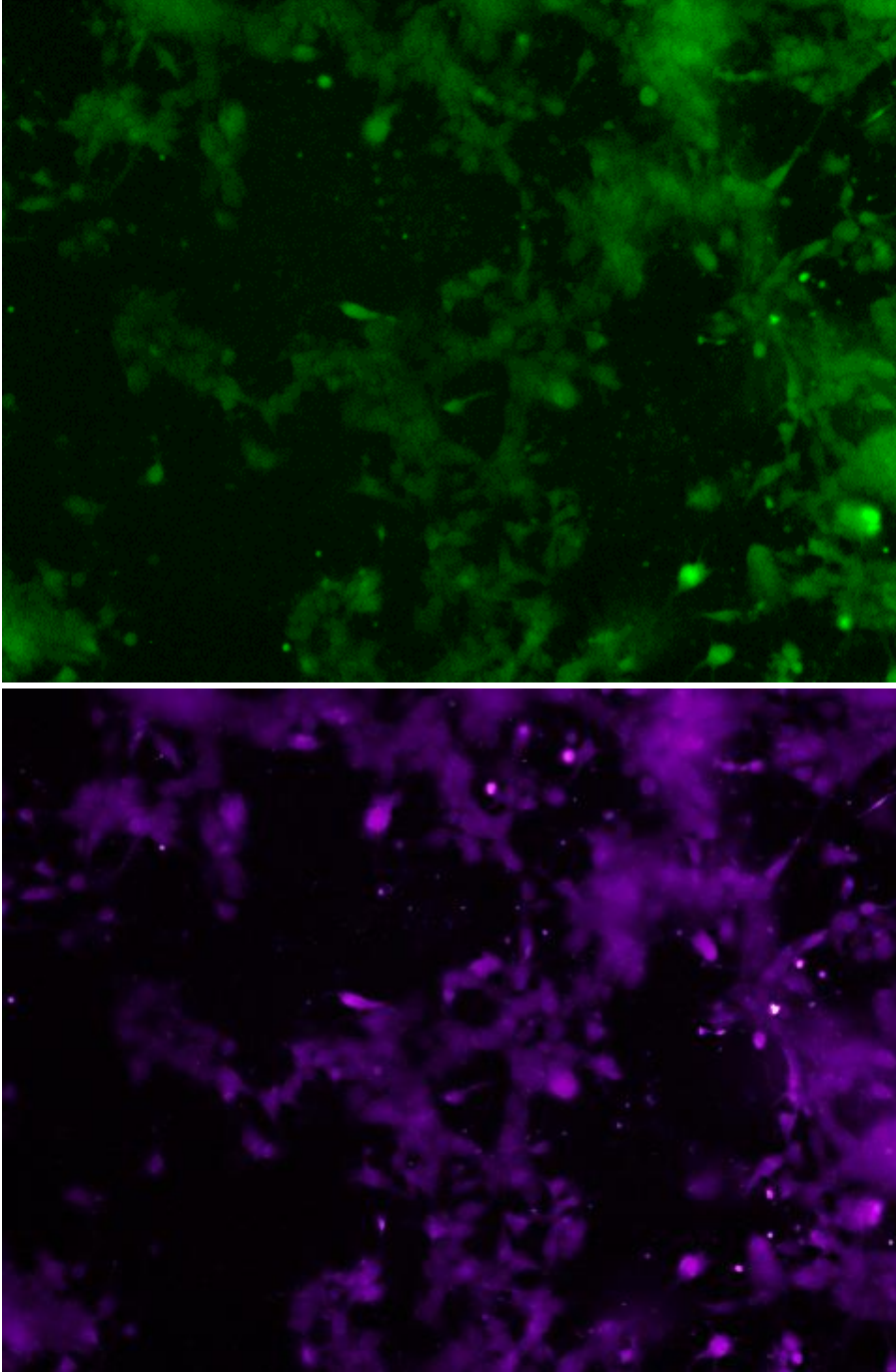


Figure S3. An image showing the cells loaded with Fura-2 at both 340nm (top) and 380nm (bottom). Both images were taken at the same exact location, using the 20x lens. The agonist used in these cells was ATP. This was an important step towards confirming whether or not the cell line can be used for Fura-2 staining.

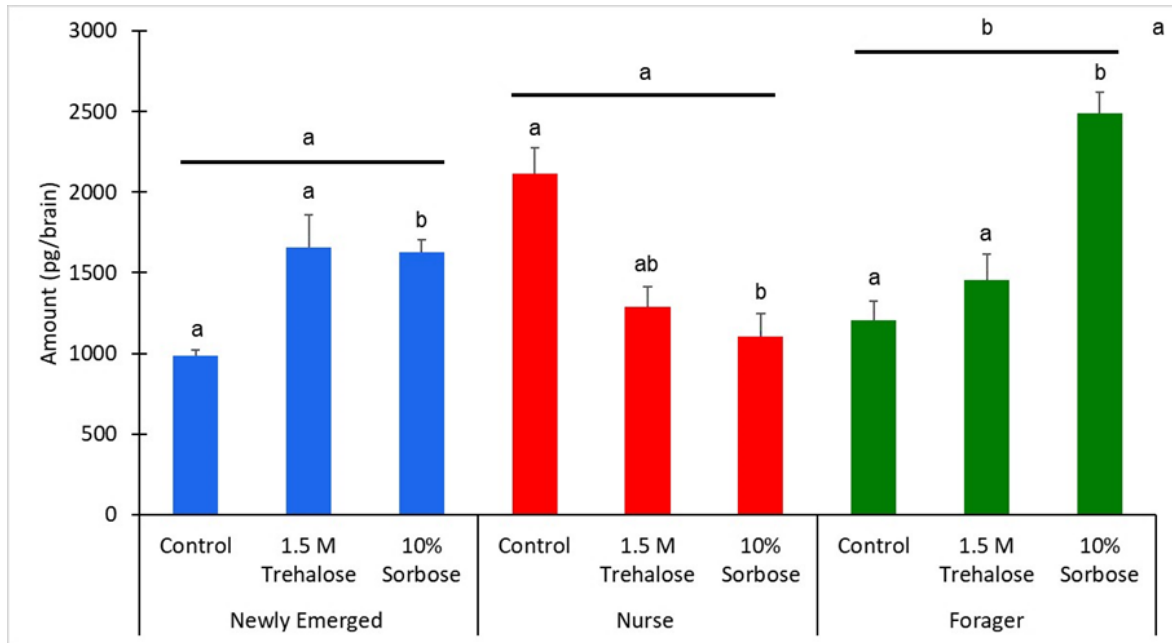


Figure S5. The biogenic amine levels on a per brain basis of Octopamine across newly emerged (blue), nurse (red), and forager bees (green). Each age group was treated with Ringer's (control), trehalose 1.5M and Sorbose 10%. The bars represent the mean. The error bars represent standard errors. The sample sizes are indicated above each bar. The letters above each bar represent significant difference treatment combinations, while the different letters above the lines represent significant differences across the age classes at the alpha = 0.05 level.

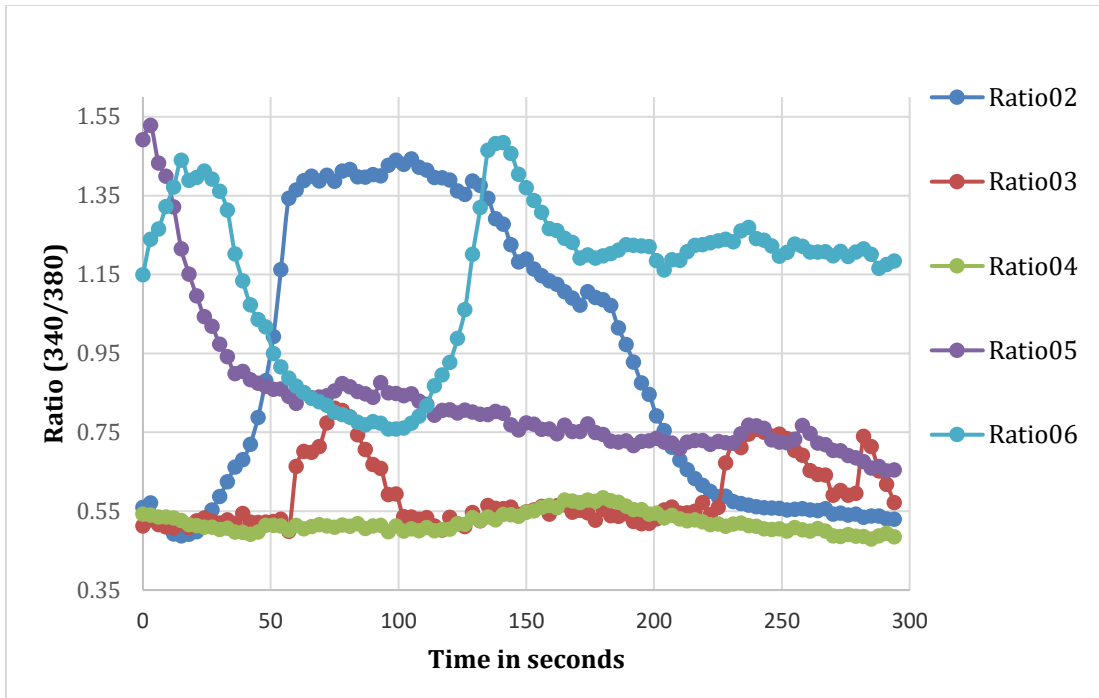


Figure S6. (A) Quantification of the signal ratio (340/380) for Fura-2 imaging. Each line corresponds to a single cell. Octopamine 1 mM (agonist) was added to the cells at 1.5 min. Replicate #1

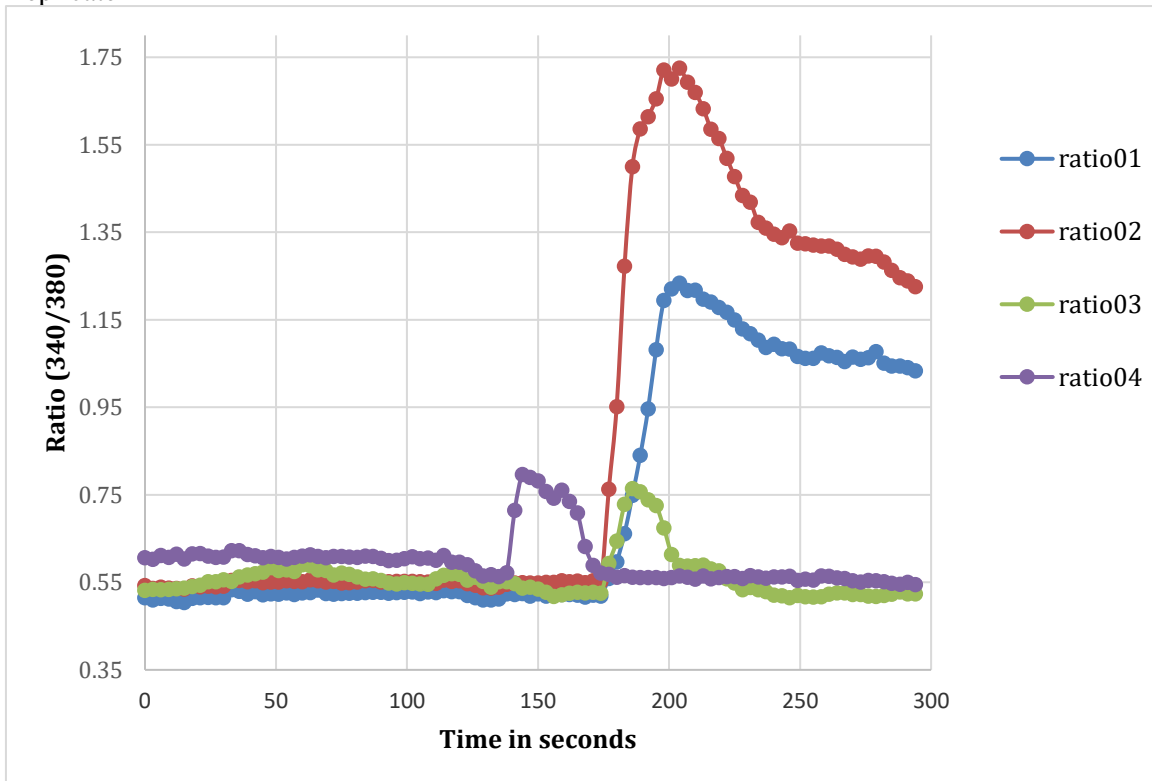


Figure S6 (B) Quantification of the signal ratio (340/380) for Fura-2 imaging. Each line corresponds to a single cell.

Octopamine 7 mM (agonist) was added to the cells at 1.5 min. Replicate #1

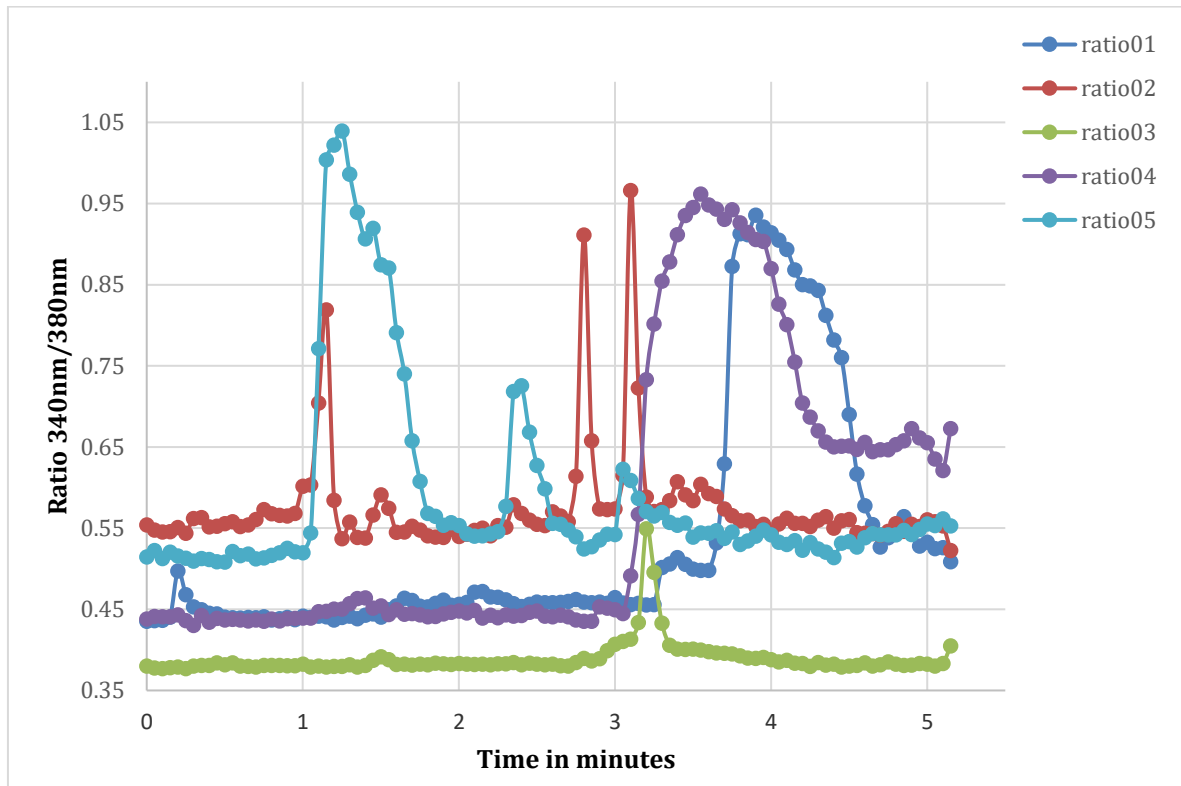


Figure S6 (C) Quantification of the signal ratio (340/380) for Fura-2 imaging. Each line corresponds to a single cell.

Octopamine 7 mM (agonist) was added to the cells at 1.5 min. Replicate #2

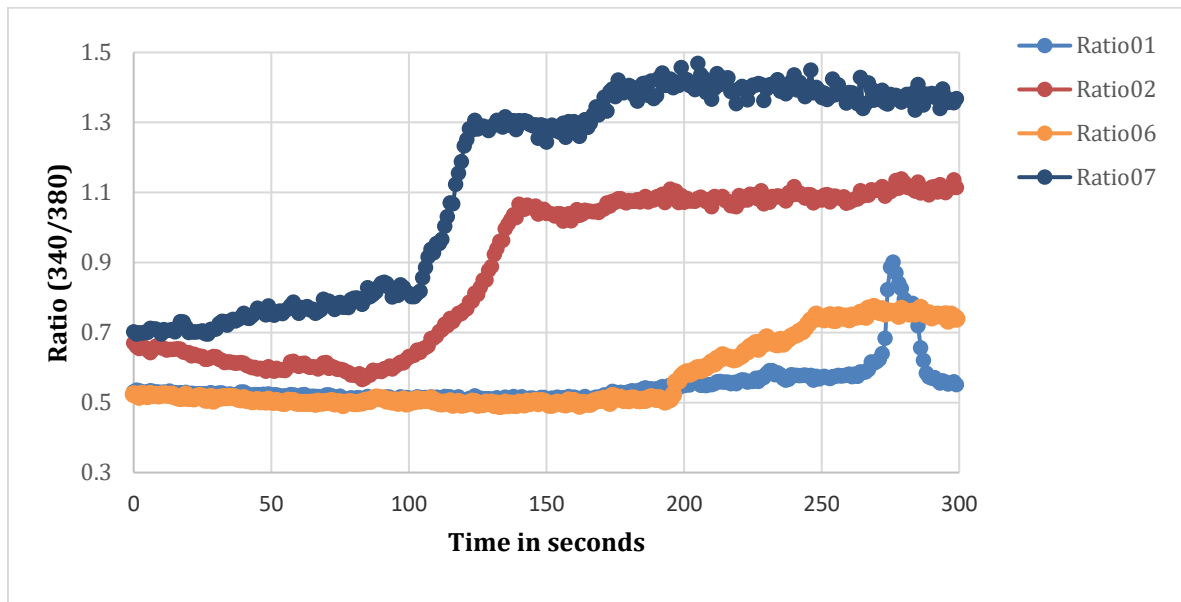


Figure S6 (D) Quantification of the signal ratio (340/380) for Fura-2 imaging. Each line corresponds to a single cell.

Octopamine 7 mM (agonist) was added to the cells at 1.5 min. Replicate #3

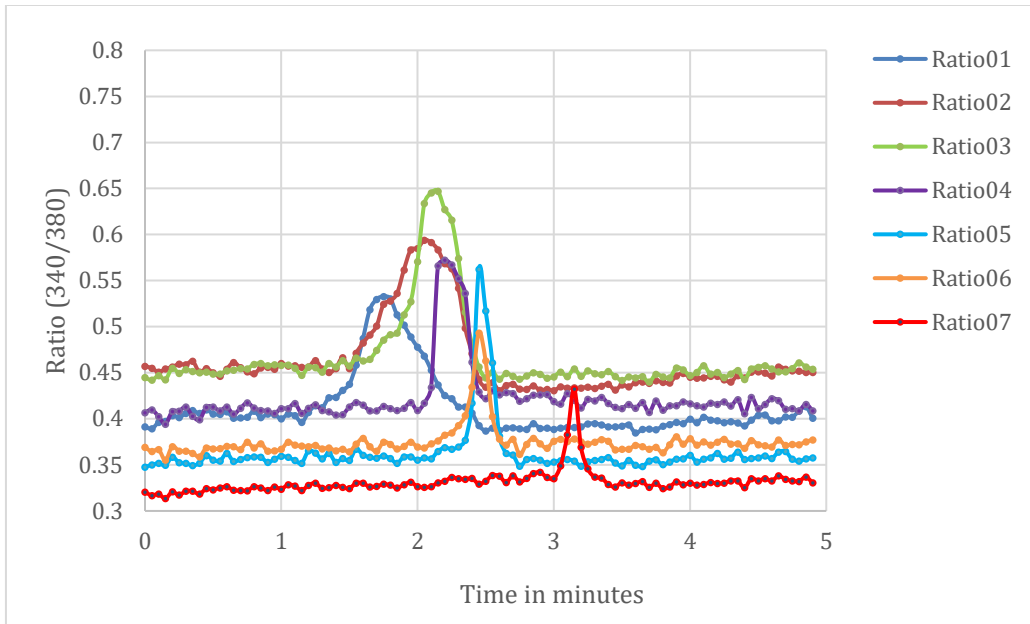


Figure S6 (E) Quantification of the signal ratio (340/380) for Fura-2 imaging. Each line corresponds to a single cell.
Octopamine 7 mM (agonist) was added to the cells at 1.5 min. Replicate #4